Erratum to "An Exact Approach for Solving Pickup-and-Delivery Traveling Salesman Problems with Neighborhoods"

Cai Gao[1], Ningji Wei[2], Jose L. Walteros[1*]

[1]Department of Industrial and Systems Engineering, University at Buffalo, The State University of New York
[2]Department of Industrial, Manufacturing and Systems Engineering, Texas Tech University

Abstract

The purpose of this erratum is to correct an error in the paper [Gao, C., Wei, N., and Walteros, J. L. (2023). An Exact Approach for Solving Pickup-and-Delivery Traveling Salesman Problems with Neighborhoods, *Transportation Science*, 57(6):1560–1580]. Specifically, the original paper proposed a generalized Benders decomposition approach that may generate invalid optimality cuts. In this document, we present a corrected version of the methodology, along with an extension to address cases in which the neighborhoods are nonconvex. In addition, we introduce a new pruning constraint to dynamically reduce the solution space. Finally, we update the computational experiments reported in Tables 2 and 3 of the original paper by applying the corrected methodology.

1 Background

The following formulation (i.e., Formulation (5) in the original paper) was introduced to model the pickup-and-delivery traveling salesman problem with neighborhoods (PDTSPN).

$$\min_{u_{ij}\in\{0,1\}} \quad \sum_{i\neq j\in I_0} \bar{z}_{ij}u_{ij} + \theta \tag{1a}$$

$$\text{s.t.} \quad \sum_{j\in I_0, j\neq i} u_{ij} = 1, \qquad \forall\, i \in I_0, \tag{1b}$$

$$\sum_{j\in I_0, j\neq i} u_{ji} = 1, \qquad \forall\, i \in I_0, \tag{1c}$$

$$\sum_{i,j\in I', i\neq j} u_{ij} \leq |I'| - 1, \qquad \forall\, I' \subsetneq I_0, |I'| \geq 2, \tag{1d}$$

$$\sum_{(i,j)\in T} u_{ij} \leq |T| - 1, \qquad \forall\, T \in \mathcal{T}, \tag{1e}$$

$$\theta \geq \Phi(u), \tag{1f}$$

$$\theta \geq 0, \tag{1g}$$

where each neighborhood $U_i := \{x \mid f_i(x) \leq 0\}$ is assumed to be a compact set in $\mathbb{R}^2$ with nonempty interior, $\bar{z}_{ij}$ is a precomputed lower bound on the distance between neighborhoods U_i and U_j, and

*Corresponding author: Phone: 716-645-8876; Fax: 716-645-3302; Address: 413 Bell Hall, Buffalo, NY 14260; Email: josewalt@buffalo.edu

the binary variables $u = \{u_{ij} \mid i, j \in I_0 \text{ and } i \neq j\}$ indicate whether neighborhood U_i appears immediately before neighborhood U_j in the selected tour. Furthermore, $\Phi(u)$ is a function that captures the difference between the minimum tour length for the visiting sequence defined by u and the lower bound $\sum_{i \neq j \in I_0} \bar{z}_{ij} u_{ij}$, defined as

$$\begin{aligned} \Phi(u) := \min_{x_i \in \mathbb{R}^2, z \in \mathbb{R}} & \sum_{i \neq j \in I_0} u_{ij}(z_{ij} - \bar{z}_{ij}) \\ \text{s.t. } & f_i(x_i) \leq 0, \quad \forall i \in I_0 \\ & \|x_i - x_j\|_2 \leq z_{ij}, \quad \forall i \neq j \in I_0. \end{aligned} \tag{2}$$

To solve (1), the original paper proposed a decomposition approach designed to generate generalized Benders cuts (GBCs). The proposed approach was shown to be incorrect by Araya et al. (2025), who demonstrated that the GBCs generated by our methodology may cut feasible solutions. After analyzing the explanation provided in their manuscript, we identified the source of the error and developed a corrected version of the proposed methodology.

In what follows, we provide an alternative explanation of why the original GBCs are invalid and then present a new derivation that correctly generates valid GBCs, thereby addressing the issues identified by Araya et al. (2025).

2 Invalid GBCs

In the original decomposition, a *master problem* was defined by replacing (1f) with a set of inequalities derived sequentially by solving the *subproblem* (2). Specifically, since the subproblem is convex and Slater's condition holds due to the nonempty interior assumption, the Lagrangian dual associated with (2) satisfies strong duality for every feasible u. That gives,

$$\Phi(u) = \sup_{\pi \leq 0, \mu \leq 0} \inf_{x,z} \sum_{i \neq j \in I_0} u_{ij}(z_{ij} - \bar{z}_{ij}) - \sum_{i \in I_0} \pi_i f_i(x_i) - \sum_{i,j \in I_0, i \neq j} \mu_{ij}(\|x_i - x_j\|_2 - z_{ij}). \tag{3}$$

Let (π^*, μ^*, x^*, z^*) be the saddle point of the above problem. Note that the last two summations become zero at the saddle point due to complementary slackness, which gives

$$\Phi(u) = \sum_{i \neq j \in I_0} (z^*_{ij} - \bar{z}_{ij}) u_{ij}.$$

The incorrect argument in the original paper arises from suggesting that one can add the following cuts to the master problem to bound $\Phi(u)$ from below.

$$\theta \geq \sum_{i \neq j \in I_0} (z^*_{ij} - \bar{z}_{ij}) u_{ij}. \tag{4}$$

This would be correct if $\Phi(u)$ were convex on u. However, in our case, $\Phi(u)$ is in fact concave, since (2) is the minimum over a set of linear functions on u. This renders the originally proposed cut (4) invalid and, hence, Proposition 3 incorrect.

From the perspective of generalized Benders decomposition (GBD), it can be seen that our original GBD implementation fails to satisfy property (P) (Geoffrion 1972) due to the structure of the objective function in (2), which, according to Bagajewicz and Manousiouthakis (1991), may cause the methodology to converge to suboptimal solutions.

In the following section, we show that standard linearization techniques can be applied to obtain an alternative formulation of $\Phi(u)$ in which the objective function and constraints are separable in u, and (x, z). As a result, the proposed reformulation not only satisfies property (P) but also remains convex in x and z under the given assumptions. This development also provides a positive answer to the question posed by Araya et al. (2025) regarding whether GBD can be applied to solve the TPSN and its variants.

3 Corrected GBC for Convex Regions

Assume each convex region $U_i = \{x \mid f_i(x) \leq 0\}$ is conic representable as $A_i x_i + b_i \in \mathcal{C}_i$ for some convex and closed cone $\mathcal{C}_i$. Applying standard linearization techniques for the bilinear terms $w_{ij} = u_{ij}(z_{ij} - \bar{z}_{ij})$ over (2), we obtain the following reformulation:

$$\Psi(u) := \min_{x,z,w} \sum_{i \neq j \in I_0} w_{ij} \tag{5a}$$

$$\text{s.t. } w_{ij} \geq 0, \quad \forall i \neq j \in I_0 \tag{5b}$$

$$w_{ij} - z_{ij} \geq -(\bar{z}_{ij} + (\hat{z}_{ij} - \bar{z}_{ij})(1 - u_{ij})), \quad \forall i \neq j \in I_0 \tag{5c}$$

$$A_i x_i + b_i \in \mathcal{C}_i, \quad \forall i \in I_0 \tag{5d}$$

$$\|x_i - x_j\|_2 \leq z_{ij}, \quad \forall i \neq j \in I_0, \tag{5e}$$

where $\hat{z}_{ij}$ is some upper bound of $\max_{x_i \in U_i, x_j \in U_j} \|x_i - x_j\|_2$.

A simple upper bound can be obtained by outer-approximating U_i and U_j with polygons (e.g., rectangles) and taking the maximum distance over all vertex pairs. This is valid since $\|x_i - x_j\|_2$ is convex in each argument: fixing x_i (resp. x_j), the maximizer over a polytope U_j (resp. U_i) is attained at a vertex, hence a vertex–vertex pair attains the maximum.

With this choice of $\hat{z}_{ij}$, $\Psi(u) = \Phi(u)$ for every binary u. Then, performing a conic dualization with $(\pi, \gamma, \alpha, (\beta, \tau))$ as the dual variables associated with (5b)–(5e) gives,

$$\Psi(u) := \max_{\alpha,\beta,\tau} \sum_{i \neq j \in I_0} -(\bar{z}_{ij} + (\hat{z}_{ij} - \bar{z}_{ij})(1 - u_{ij}))\, \tau_{ij} - \sum_{i \in I_0} \langle b_i, \alpha_i \rangle \tag{6a}$$

$$\text{s.t. } \sum_{j \neq i} (\beta_{ji} - \beta_{ij}) - A_i^\intercal \alpha_i = 0, \quad \forall i \in I_0 \tag{6b}$$

$$\alpha_i \in \mathcal{C}_i^*, \quad i \in I_0 \tag{6c}$$

$$\|\beta_{ij}\|_2 \leq \tau_{ij}, \quad \forall i \neq j \in I_0 \tag{6d}$$

$$\tau \leq 1, \tag{6e}$$

where $\mathcal{C}_i^*$ is the dual cone of $\mathcal{C}_i$. Since each region U_i is assumed to contain an interior point x_i^0, choosing z_{ij}^0 and w_{ij}^0 sufficiently large yields a strictly feasible point (x^0, z^0, w^0) for (5). Hence, Slater's condition holds, and strong duality follows. Moreover, since $\Psi(u)$ is the pointwise maximum of a family of affine functions in u, it is convex in u. Therefore, whenever a dual optimal solution $(\alpha^*, \beta^*, \tau^*)$ is obtained, adding the following GBC cut

$$\theta \geq \sum_{i \neq j \in I_0} -(\bar{z}_{ij} + (\hat{z}_{ij} - \bar{z}_{ij})(1 - u_{ij}))\, \tau_{ij}^* - \sum_{i \in I_0} \langle b_i, \alpha_i^* \rangle \tag{7}$$

yields an exact master–subproblem approach for the convex TSPN problem.

3.1 A Pruning Cut for Enhancement

Since each subproblem returns the length of a feasible visiting sequence, let $\eta \geq 0$ denote the incumbent best length. Whenever η is improved, we update the following pruning cut in the master problem

$$\sum_{i \neq j \in I_0} \bar{z}_{ij} u_{ij} \leq \eta, \tag{8}$$

which discards unpromising visiting sequences.

4 Extension to Non-Convex Regions

The following nonlinear region representation was introduced in Section 4.3 of the original paper

$$x = \sum_{j \in [m]} \left(\lambda_j \left(v_j - v_{\iota(j)} \right) + \phi_j v_{\iota(j)} \right), \tag{9a}$$

$$\sum_{j \in [m]} \phi_j = 1, \tag{9b}$$

$$\lambda_j \leq \phi_j, \ \forall j \in [m], \tag{9c}$$

$$\lambda_j \geq 0, \phi_j \in \{0, 1\}, \ \forall j \in [m], \tag{9d}$$

where $\iota(j)$ gives the subsequence vertex of j in the given boundary sequence

$$v_1 \to v_2 \to \cdots \to v_m \to v_1.$$

Thus, when ϕ is binary, the point $x \in \mathbb{R}^2$ is constrained to lie on the closed loop formed by the sequence of line segments connecting consecutive vertices. Moreover, relaxing ϕ to $[0, 1]$ yields $\text{conv}(\{v_j\}_{j \in [m]})$. Indeed,

$$x = \sum_{j \in [m]} \lambda_j v_j + \sum_{j \in [m]} (\phi_j - \lambda_j) \, v_{\iota(j)},$$

with $\lambda_j \geq 0$ and $\phi_j - \lambda_j \geq 0$ by (9c)–(9d), and

$$\sum_{j \in [m]} \left(\lambda_j + (\phi_j - \lambda_j) \right) = \sum_{j \in [m]} \phi_j = 1.$$

Hence x is a convex combination of $\{v_j\}_{j \in [m]}$. Subsequently, the cut (7) remains valid for this relaxed problem but is generally not strong enough to guarantee feasibility with respect to the original non-convex regions. This motivates the following exact solution approach.

- **Step 1:** Run the standard cut-generation procedure based on $\Psi(u)$ on the relaxed problem.
- **Step 2 (optional):** At each subproblem iteration t, project the fractional variables ϕ onto a feasible (binary) choice, compute the corresponding tour length η_t, and use it to update the pruning constraint (8).
- **Step 3:** Let $\hat{u}$ be the optimal visiting sequence returned by the relaxed master–subproblem scheme. If the associated optimal boundary-selection solution $\hat{\phi}$ from the subproblem is binary, terminate and declare $\hat{u}$ optimal. Otherwise, solve the *binary* subproblem for the

fixed sequence $\hat{u}$ to obtain the true optimal length $\eta^*(\hat{u})$, update the incumbent solution and the pruning constraint (8), and add the following no-good cut to the master problem

$$\sum_{(i,j):\hat{u}_{ij}=1} u_{ij} \leq |I_0| - 1.$$

Then, repeat Steps 1 and 2.

- **Step 4:** If the master problem becomes infeasible, return the incumbent as optimal.

Since Step 1 solves the relaxed master problem to optimality, and Step 2 produces valid pruning updates by projecting the fractional subproblem solution to a feasible tour, iterating the first two steps solves the relaxed master-subproblem formulation to optimality. If the resulting subproblem solution $\hat{\phi}$ is binary, then the relaxation is tight, and $\hat{u}$ is optimal for the original problem. Otherwise, Step 3 solves the exact binary subproblem for the fixed sequence $\hat{u}$ to obtain its true sequence length $\eta^*(\hat{u})$, updates the incumbent (and the pruning constraint), and adds a no-good cut to exclude $\hat{u}$ from the master. Consequently, the algorithm either terminates upon finding an optimal sequence whose relaxation is integral from the relaxed problem, or systematically enumerates admissible sequences while tightening the incumbent bound.

Acknowledgement

The authors thank Araya et al. (2025) for spotting the invalid cuts.

References

D. Araya, G. Angulo, and M. Castro. Exact and approximate formulations for the close-enough TSP, 2025. Available at: https://optimization-online.org/?p=32840. Last visited: February, 2026.

M. Bagajewicz and V. Manousiouthakis. On the generalized benders decomposition. *Computers & chemical engineering*, 15(10):691–700, 1991.

A. M. Geoffrion. Generalized Benders decomposition. *Journal of Optimization Theory and Applications*, 10 (4):237–260, 1972.

An Exact Approach for Solving Pickup-and-Delivery Traveling Salesman Problems with Neighborhoods

Cai Gao[1], Ningji Wei[2], Jose L. Walteros[1*]

[1]Department of Industrial and Systems Engineering, University at Buffalo, The State University of New York

[2]Department of Industrial, Manufacturing and Systems Engineering, Texas Tech University

Abstract

This paper studies a variant of the traveling salesman problem called the pickup-and-delivery traveling salesman problem with neighborhoods that combines traditional pickup and delivery requirements with the flexibility of visiting the customers at locations within compact neighborhoods of arbitrary shape. We derive two optimality conditions for the problem, a local condition that verifies whether a given tour is locally optimal at the visiting points and a global condition that can be used to cut off sub-optimal regions of the neighborhoods. We model the problem as a mixed-integer nonlinear program and propose a generalized Benders decomposition to solve instances of the problem with convex and non-convex neighborhoods. Finally, we conduct extensive computational experiments to demonstrate the efficacy of our solution framework.

Keywords: pickup-and-delivery, traveling salesman problem, mixed-integer nonlinear program, close-enough traveling salesman problem, generalized Benders decomposition.

1 Introduction

Pickup-and-delivery problems refer to a class of vehicle routing problems in which vehicles are used to transport commodities or passengers from a set of origins to a set of destinations on a given transportation network (Toth and Vigo, 2002, Battarra et al., 2014). Several variations of these problems have been extensively studied over the years, addressing applications in areas such as transportation, disaster relief, and communications, among others (Berbeglia et al., 2007, 2010, Kalantari et al., 1985, Parragh et al., 2008, Ropke and Pisinger, 2006, Savelsbergh and Sol, 1995, Xu et al., 2003).

When only a single vehicle is available to conduct the transportation tasks, the given problem is commonly referred to as the *pickup-and-delivery traveling salesman problem* (PDTSP) (Kalantari et al., 1985), and, contrary to the classic TSP where the decision-maker only has to minimize the distance the vehicle must travel, the PDTSP also requires considering additional constraints posed by the relationship between the

*Corresponding author: Phone: 716-645-8876; Fax: 716-645-3302; Address: 413 Bell Hall, Buffalo, NY 14260; Email: josewalt@buffalo.edu

pickup and delivery orders and often a capacity constraint (Gendreau et al., 1999, Hernández-Pérez and Salazar-González, 2004a, Kalantari et al., 1985, Renaud et al., 2000).

In this study, we focus on a generalization of PDTSP called the *pickup-and-delivery traveling salesman problem with neighborhoods* (PDTSPN), where the transactions between the vehicle and the customers occur at points located within specific neighborhoods (i.e., compact regions embedded in $\mathbb{R}^2$) defined for each customer. As such, instead of visiting predefined locations specified by the customers, the vehicle requires determining a shortest closed tour that intersects with each customer's neighborhood at least once while satisfying their corresponding pickup or delivery requirements and often a capacity constraint.

In practice, PDTSPN can model routing problems with some level of flexibility in the choice of meet-up locations, for example, in cases where the transactions can be made remotely (e.g., when the transported commodity consists of data, which is transferred wirelessly) or in cases where the customers are willing to move away from their location and meet with the vehicle at more convenient locations for the distribution plan. Furthermore, considering that the neighborhoods may overlap, a vehicle following an optimal tour may then meet with multiple customers at the same location, thereby potentially reducing the total distance traveled.

In what follows, we review the relevant literature associated with PDTSPN and provide two motivating applications of transportation and distribution problems that can be modeled as such.

1.1 Literature review

Because of the absence of papers addressing this specific variation of the TSP, we focus on studies on its two main individual components. We begin our discussion with an overview of general developments on the PDTSP, followed by a survey that addresses the TSP with neighborhoods (TSPN).

1.1.1 PDTSP literature.

In general, most pickup-and-delivery problems partition the customers into two sets: the *demand customers*, which are the ones requesting commodities to be delivered, and the *supply customers*, which are the ones requiring commodities to be picked up. Furthermore, depending on the precedence relationship between the demand and supply customers, there are three main categories often used to classify most variations of PDTSP: the *one-to-many-to-one (1-M-1)*, the *many-to-many (M-M)*, and the *one-to-one (1-1)* (Toth and Vigo, 2002) problems. In the 1-M-1 version, all the commodities delivered to the demand customers must come directly from the depot, and all the commodities collected from the supply customers must be transported back to the depot. This problem is also called the TSP with pickups and deliveries in Mosheiov (1994) and the TSP with delivery and backhauls in Anily and Mosheiov (1994). In the M-M version, there is only one type of commodity that is collected from the supply customers and delivered to the demand customers. This version is also known as the one-commodity PDTSP (Hernández-Pérez and Salazar-González, 2004a). Finally, in the 1-1 version, there is a one-to-one correspondence between the supply and the demand customers. i.e., the commodities collected from each supply customer are designated to be delivered to a specific demand customer. When the number of commodities to be transported between each pair of customers is a single unit, this problem is also called the *single vehicle many-to-many dial-a-ride problem* (Psaraftis, 1983). We now address specific developments related to these three variations.

To the best of our knowledge, Mosheiov (1994) was the first to study the 1-M-1 PDTSP. In this paper, the author proposed an approximation algorithm with a worst-case performance ratio of 2.5 that works under the assumption that the distance matrix is symmetric. Subsequently, Anily and Mosheiov (1994) improved this bound to 2 by using a minimum-spanning-tree-based approximation algorithm derived from the well-known Christophides heuristic for TSP (Christofides, 1976). It is important to note that, under some considerations, if the problem allows customers to have both types of orders (suply and demand), the optimal tour may visit some customers more than once. While this case is out of scope for this paper, we refer the interested reader to the work by Gribkovskaia et al. (2007), where each customer is allowed to be visited once for a combined pickup-delivery operation or twice for performing the two operations separately.

For the M-M PDTSP case, Hernández-Pérez and Salazar-González (2004a) were the first to tackle this problem, proposing a branch-and-cut algorithm able to solve instances with up to 40 customers to optimality. To solve larger instances within a reasonable time, Hernández-Pérez and Salazar-González (2004b) proposed two heuristics, one based on 2-*opt* and 3-*opt* local moves, and the other based on a branch-and-cut procedure. With these heuristics, the authors were able to solve instances with up to 500 customers. Since then, other heuristic and metaheuristic methods have been successfully applied to solve the problem in recent years (Mladenović et al., 2012, Hernández-Pérez et al., 2009, Zhao et al., 2009).

As for the 1-1 PDTSP version, Kalantari et al. (1985) were the first to solve this problem under the name *TSP with pickup and delivery* (TSPPD). The authors proposed an exact branch-and-bound algorithm able to solve instances with up to 31 customers. In recent years, Dumitrescu et al. (2010) analyzed the polyhedral structure of the problem and proposed a branch-and-cut algorithm with multiple cut separation subroutines.

In addition to the standard version of 1-1 PDTSP, there are other interesting variants worth mentioning: the PDTSP with last-in-first-out (LIFO) or first-in-first-out (FIFO) loading policies (Cordeau et al., 2010b,a), the PDTSP with handling costs (Veenstra et al., 2017, Qu and Bard, 2015), and the TSP with dynamic pickups and deliveries (O'Neil and Hoffman, 2017). Also, while our previous discussion was focused on the single-vehicle version of the problem (i.e., the TSP version), we note that other developments exist for solving the problem with multiple vehicles. We refer the interested reader to the surveys found in Toth and Vigo (2002).

1.1.2 TSPN literature.

The TSPN is a generalization of the classic TSP, where the nodes representing the customers are replaced with compact sets called neighborhoods or regions. To the best knowledge Arkin and Hassin (1994) were the first to introduce this problem with the name *geometric covering salesman problem*. In this study, the authors provide several $O(1)$-approximation algorithms for cases where the neighborhoods have specific shapes, such as parallel line segments of equal lengths, or regions that are generated from the same type of convex polygon. More recently, Dumitrescu and Mitchell (2003) extended and improved these results for neighborhoods with similar diameters, unit disks, and straight lines. In particular, the authors proposed a polynomial-time approximation scheme (PTAS) for the problem with neighborhoods that are disjoint disks with similar diameters. For TSPN with arbitrary compact shapes, Mata and Mitchell (1995) provided a framework that gives an $O(\log k)$-approximation algorithm with time complexity $O(n^5)$, where k stands for the number of polygonal neighborhoods and n is the total number of vertices of all the polygons. More recently, Gudmundsson and Levcopoulos (1999) proposed an algorithm that improves such complexity to

$O(n^2 \log n)$.

In some literature, TSPN is alternatively called the *close-enough traveling salesman problem* (CETSP) (Behdani and Smith, 2014, Gulczynski et al., 2006). In CETSP, the neighborhoods are often defined as disks in a two-dimensional space or closed balls in a three-dimensional space (Coutinho et al., 2016, Carrabs et al., 2017, Wang et al., 2019). This problem has been generalized for compact neighborhoods of arbitrary shapes in (Behdani and Smith, 2014), where the authors proposed two different discretization schemes to approximate any compact neighborhoods and developed three mixed-integer programming formulations based on these discretization schemes to provide lower bounds for the problem. Carrabs et al. (2017) further improved the lower and upper bounds by presenting a new discretization scheme, which is capable of solving instances with up to 30 neighborhoods. Coutinho et al. (2016) proposed an efficient exact approach based on a combinatorial branch-and-bound algorithm that uses a second-order conic program as a subroutine. In addition to exact approaches, several efficient heuristics have been developed to solve the problem as well (Gulczynski et al., 2006, Yuan et al., 2007, Mennell, 2009, Wang et al., 2019).

1.2 Motivating Examples

1.2.1 Data collection and distribution.

While the origins of the TSPN can be traced back to the 90s, some variations of this problem have gained traction in recent years, spurred by the emergence of unmanned aerial vehicles (UAV) as viable tools to conduct transportation and communications tasks (Renaud et al., 2000, Wang et al., 2019). Thanks to recent technological advancements and decreasing production costs, UAVs are rapidly becoming invaluable for military and civilian logistics, finding multiple uses across several domains (Dell'Amico et al., 2021, Murray and Chu, 2015, Agatz et al., 2018). However, despite their benefits in terms of accessibility and flexibility, their maximum payload and flying range are often two limiting factors that should be considered when using them for such purposes.

In general, most applications of TSPN and its variations aim to optimally route a UAV with mounted sensors for collecting information while taking advantage of wireless communication protocols (e.g., RFID). Applications such as meter-reading and distant-monitoring logistics (Wang et al., 2019) are the prototypical examples explored in most TSPN papers, as considerations regarding the UAV's payload or different types of customer interactions (like pickups and deliveries) are not required in such cases. However, in more complex scenarios that require the exchange of large amounts of data between multiple actors, other important factors come into play that require modeling such routing problems differently.

One notable example arises when solving intelligence, surveillance, and reconnaissance problems in remote or denied areas (Emami et al., 2020, Ono et al., 2016, Li et al., 2019, Wei et al., 2021). In these problems, a collection of sensors (mobile or static) are placed to gather information from multiple targets. Without the support of a communication network to directly transfer the collected data to their base stations, the sensors often depend on UAVs (a.k.a, relays) that are routinely sent to follow collection routes to interact with them. In this particular context, in addition to the precedence requirements of the relay's visiting sequence given by the sensor/base station pairings, the maximum payload of the relay also imposes a major restricting factor when transferring several types of data, such as high-definition video. This is because the weight of the data storage hard drives limits the number of them that can be mounted on the relay. Considering that the data from each sensor may need to be delivered to one of several base stations in the area and the fact that both

the sensors and relays can transfer data remotely, some of these the relay's routing problems can be modeled as a 1-1 PDTSPNs. See Figure 1 for a pictorial example of this data collection and distribution operation.

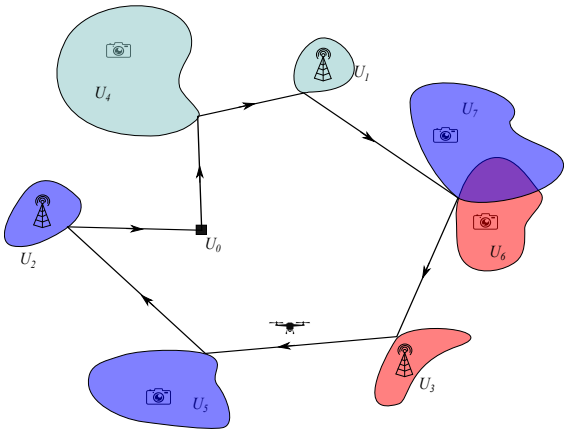

Figure 1: Relay routing for data collection and distribution. Sensors (depicted as cameras) and base stations (depicted as antennas) are each located in one of seven regions. The shape of the regions describes some form of proximity range required for the relay and sensors to exchange data. Irregular shapes may be the result of obstacles and other potential interference sources. Sensors and base stations of the same color indicate to which base station the relay must deliver the data collected by which sensors. The relay is dispatched from its base at location U_0 to conduct the data distribution operation. The closed tour with arrows provides a feasible routing plan.

1.2.2 Primary healthcare for tribal populations.

Primary healthcare delivery for tribal communities has been a pressing societal problem over the last few decades (Belongia, 1988, Mavalankar, 2016, Ramalingareddy, 2016). In multiple countries like India, Tanzania, South Africa, Colombia, Peru, and Bolivia, local healthcare organizations constantly seek new opportunities to improve access to medical services for isolated populations. Unfortunately, the lack of nearby medical facilities and transportation services are some of the primary hurdles that severely limit the quality and regularity of the services provided to these communities (Mavalankar, 2016).

Among the different available programs, one that has been regularly implemented consists of deploying medical crews to set temporal healthcare camps in tribal lands to provide medical services to nearby populations or assist medical personnel living in surrounding areas (Belongia, 1988). Given the terrain conditions, such visitation programs are often conducted via helicopter or small truck convoys, thus limiting the number of medical supplies the medical crews can carry with them—particularly those requiring refrigeration.

From the logistics perspective, the routing problem of a medical crew following this type of visitation program can be modeled as an M-M PDTSPN, where each isolated community and local personnel comprise the problem's customers. Besides the medical services, each customer generally requires some medical supplies to be delivered, such as vaccines or antibiotics, and other items to be returned, like blood samples to be analyzed back at the medical facilities, resulting in the pickup and delivery component of the problem. The regions in this particular context describe the nearby areas sufficiently close for the populations to travel and meet the medical crews. As the visitation journey progresses, the temporal camp is then moved and placed at the intersections between the planned route and corresponding regions. Furthermore, as was the case for the UAV example, each region can be defined, excluding potential areas where the temporal camp

cannot be placed.

Besides the aforementioned examples, other applications in military operations include problems involving the simultaneous delivery of supplies and extraction of wounded personnel, among others.

1.3 Contributions

Despite the broad interest in the PDTSP and TSPN, little work has been devoted to PDTSPN, which considers the two fundamental components of the other two problems simultaneously. In this paper, we are interested in addressing this gap by studying exact methods for solving the PDTSPN. The main contributions of this paper follow.

1. We derive two optimality conditions for PDTSPN with compact neighborhoods that have arbitrary shapes. The first condition characterizes whether a given tour is locally optimal at the visiting point of each neighborhood. For the second condition, we identify a certain type of half-plane denoted as boundary-projection-closed separator which contains all the "non-redundant" optimal tours. Then, we show that the intersection of all these separators, defined as the domination hull, can be used to cut off sub-optimal regions of the neighborhoods. We also develop a binary-search-based algorithm to approximate the domination hull efficiently.

2. We propose a mixed-integer nonlinear programming (MINLP) formulation to solve PDTSPN instances with convex and non-convex neighborhoods and introduce a cut-generation implementation that produces exact optimal solutions. Our approach is based on a generalized Benders decomposition that iterates between two models, a master problem that identifies the feasible visiting order of the tour and a subproblem that computes the optimal visiting locations of the tour given the visiting order provided by the master and generates optimality Benders cuts. We show how to adapt our approach to tackle instances of PDTSPN with several supply-demand precedence relationships including the 1-1, 1-M-1, and M-M versions.

3. We conduct an extensive set of computational experiments to test the proposed solution approach on a wide variety of instances. We analyze the performance of our approach and discuss some observations and possible adaptations.

The rest of the paper is organized as follows. In Section 2, we give an exact account of the problem setting and assumptions. In Section 3, we study two optimality conditions for PDTSPN, which can also be implemented to solve other variants of TSPNs with general shapes. In Section 4, we propose a mixed-integer nonlinear programming formulation to solve PDTSPN. In Section 5, we conduct a battery of computational experiments to test our solution approach. Finally, in Section 6, we conclude the paper and offer further insights. To streamline the discussion, we provide all the mathematical proofs in Appendix 7.

2 Problem Description

For the sake of simplicity, we limit the following exposition to the M-M version of PDTSPN. However, in Section 4, we will describe how to apply the proposed framework to solve instances with other types of precedence relationships.

2.1 Preliminaries

Let $I_0 = \{0, 1, \cdots, n\}$ be an index set and $\mathcal{U} = \{U_i\}_{i \in I_0}$ be a given collection of compact sets in $\mathbb{R}^2$ that may overlap. In particular, U_0 is assumed to be a single point p_0, which we call the depot. Assigned to each non-depot neighborhood U_i, there is either a positive supply of commodities s_i to be collected from or a positive demand of commodities d_i to be delivered to. We denote I_s and I_d the index sets for the supply and demand neighborhoods. For variations of PDTSPN other than the M-M, if there is a neighborhood that has both supply and demand orders, we create two copies of the same neighborhood and add one index to both I_s and I_d representing each copy. This ensures that the pair of index sets I_s and I_d induces a partition of set $I = I_0 \setminus \{0\}$. A vehicle with capacity c is assumed to be dispatched from the depot U_0 to collect or deliver the commodities to each neighborhood.

For the following presentation, we first require to adapt some common TSP concepts. In particular, since traditional TSP problems are defined over graphs where each customer is characterized by a node, every feasible tour is represented by a Hamiltonian cycle on the graph. On the other hand, since PDTSPN is defined over compact area in $\mathbb{R}^2$, where feasible tours may traverse each neighborhood passing by multiple points, this concept must be adapted accordingly.

Definition 1 (Neighborhood Visit)**.** *A visit to a neighborhood U_i is assumed to occur if the vehicle enters the neighborhood and either collects or delivers a positive amount of commodities at a certain point $p_i \in U_i$.*

Thus, a vehicle passing by a neighborhood without collecting or delivering any commodity is not considered a visit.

Definition 2 (Hamiltonian PDTSPN Tour)**.** *Given a collection of neighborhoods $\mathcal{U} = \{U_i\}_{i \in I_0}$ with positive supplies or demands, a PDTSPN tour is assumed to be Hamiltonian if it is a closed tour that starts at the depot U_0 and visits each non-depot neighborhood exactly once.*

Under this settings, the *pickup-and-delivery traveling salesman problem with neighborhoods* (PDTSPN) seeks for a shortest Hamiltonian tour that satisfies all the supply and demand requirements (see Figure 2 for an example).

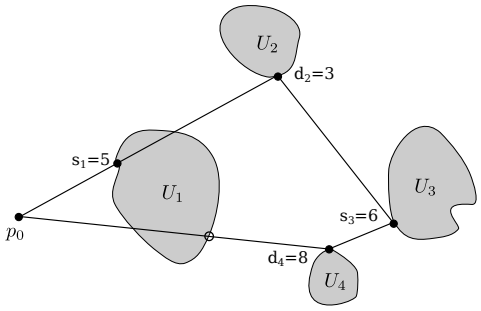

Figure 2: A M-M PDTSPN instance with $|I| = 4$ neighborhoods and one depot. A feasible tour is constructed by selecting a point (solid black dot) from each neighborhood. In this solution, the vehicle first collects 5 units at neighborhood U_1, delivers 3 units to U_2, continues to pick up 6 units at U_3, then delivers all 8 units to U_4, before returning to the depot p_0. Notice that the hollow dot at the boundary of U_1 along with all the subsequent points that intersect that neighborhood are not counted as visits to U_i.

Throughout the paper, we have the following assumption.

Assumption 1. A PDTSPN instance satisfies the following conditions:

(i) The total supply is equal to the total demand: $\sum_{i \in I_s} s_i = \sum_{i \in I_d} d_i$.

(ii) The vehicle capacity c is greater or equal to the total supply $\sum_{i \in I_s} s_i$.

Condition (i) ensures that the supply and demand requirements can be satisfied. This is assumed w.l.o.g because the depot U_0 can always be used to adjust the deficit or surplus of commodities. Condition (ii) ensures that there exists a tour that visits each neighborhood at most once. Both conditions suffice to guarantee the existence of an optimal Hamiltonian tour (see Proposition 1).

2.2 Solution Characterization

Without Assumption 1, the optimal solution of PDTSPN may not be Hamiltonian. This can occur, for instance, if capacity c is strictly less than s_i for some $i \in I$. In such a case, the vehicle has to visit neighborhood i more than once to satisfy that supply requirement. Moreover, notice that, even under the assumption that $c \geq s_i$ for all $i \in I_s$ and $c \geq d_i$ for all $i \in I_d$, it is possible to construct instances that require visiting at least one neighborhood more than once. Consider, for example, an instance with three demand customers, all with $d_i = 5$, five supply customers, all with $s_i = 3$, and a vehicle with capacity $c = 5$. In such a case, it is easy to see that the vehicle cannot satisfy the supply-demand requirements by visiting all the neighborhoods exactly once.

The following proposition shows that Assumption 1 ensures there is always a Hamiltonian solution to the problem. While the result of this proposition is quite intuitive, we provide the proof for the sake of completeness. Furthermore, the proof is given for the M-M case; however, we note that a sufficient capacity on the vehicle always leads to a Hamiltonian optimal tours even for other versions, as visiting the same location multiple times only lengthens the total distance.

Proposition 1. *A PDTSPN instance that satisfies Assumption 1 admits an optimal tour that visits each neighborhood exactly once. Moreover, such tour is a shortest Hamiltonian tour where the visits take place at some set of points $\{p_i\}_{i \in I}$, where $p_i \in U_i$ for all $i \in I$.*

According to Proposition 1, we only need to focus on Hamiltonian tours. Let S_n be the symmetric group that contains all the permutations of the index set I, then each $\sigma \in S_n$ indicates a unique visiting order of the neighborhoods. Thus, any Hamiltonian tour that conforms with the visiting order σ can be represented by a sequence of points $(p_0, \mathbf{p})$ for some $\mathbf{p} \in \prod_{i \in I} U_{\sigma(i)}$, where $U_{\sigma(i)}$ is the ith visited neighborhood under σ. This representation allows us to model the problem as follows:

$$\min_{\sigma \in S_n} \quad \min_{\mathbf{p} \in \prod_{i \in I} U_{\sigma(i)}} HT(p_0, \mathbf{p}) \tag{1a}$$

$$s.t. \quad \sum_{j \leq i} s_{\sigma(j)} \geq \sum_{j \leq i} d_{\sigma(j)}, \quad \forall\, i \in I, \tag{1b}$$

where $HT(\cdot)$ denotes the length of the Hamiltonian tour for the visiting order given by σ. Constraint (1b) enforces that, for each subpath $p_0 \rightsquigarrow p_i$, for all $i \in I$, the amount of supplies carried by the vehicle is sufficient to satisfy all the demands up to the neighborhood i. We also note that constraints (1b) only affect the visiting order of permutation σ and do not restrict selection of visiting points $\mathbf{p}$. This implies

that selection of such points is only handled by the inner level, independently of the supplies and demands. Hence, any new developments for solving the inner problem can be used to solve other variations of TSPN as well. The following section is devoted to studying some optimality conditions for the general TSPN.

3 Optimality Conditions for TSPN Solutions

The TSPN described by Formulation (1a) can be generally expressed as the following model.

$$\min_{\sigma \in S_n, \{x_i\}_{i \in I}} \quad \sum_{i \in I \setminus \{n\}} \delta(x_{\sigma(i)}, x_{\sigma(i+1)}) + \delta(p_0, x_{\sigma(1)}) + \delta(p_0, x_{\sigma(n)}) \tag{2a}$$

$$s.t. \quad f_i(x_i) \leq 0, \quad \forall i \in I, \tag{2b}$$

where the function $\delta : \mathbb{R}^2 \times \mathbb{R}^2 \to [0, \infty)$ represents the Euclidean distance, and the functions in $\{f_i\}_{i \in I}$ define the neighborhoods. That is, for each $f_i : \mathbb{R}^2 \to \mathbb{R}^k$ for some $k \in \mathbb{N}$, the compact neighborhood U_i is described as the preimage of the non-positive orthant $U_i := \{x \in \mathbb{R}^2 \mid f_i(x) \leq 0\}$. To the authors' knowledge, this type of two-stage reformulation for CETSP problems was first introduced in Behdani and Smith (2014), where the authors studied the general CETSP problem, developed three solution approaches based on a discretization scheme, and compared their computational performances.

In general, there are many choices of functions $\{f_i\}_{i \in I}$ to describe compact regions in $\mathbb{R}^2$. For instance, they can be used to represent (a) the intersection of a set of half-planes, (b) ellipsoids, or (c) a neighborhood enclosed in line segments connecting a finite sequence of points. Given a fixed visiting order σ, different neighborhood representations induce various types of formulations: (a) produces a quadratic program with linear constraints; (b) can be formulated as a second-order cone program; (c) can be solved by the second-order conic integer program. Instead of analyzing all these variations, we are interested in deriving optimality conditions for solutions of the general TSPN, which are invariant under the specific realizations of f's. Therefore, the results that will be introduced in this section can be used to either produce valid constraints or improve subroutines for any TSPN implementation with various realizations of f's.

To keep the generality, we assume that all neighborhoods are compact in this section. Note that compact neighborhoods can still have complex topological properties: Figure 3 displays several types of compact neighborhoods. From left to right, we have a disconnected neighborhood, a disconnected neighborhood with holes, a path-connected non-convex neighborhood, and a convex neighborhood. To study neighborhoods with such general properties, we first introduce some basic geometric objects.

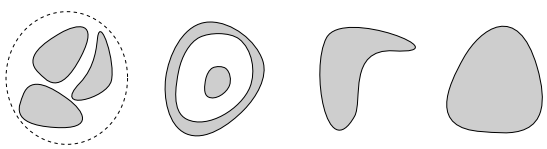

Figure 3: Neighborhoods with different topological properties.

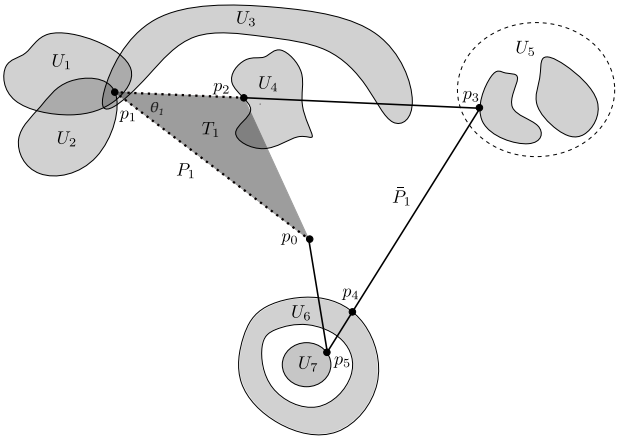

Figure 4: Neighborhood-related objects: T_1 is the shaded triangle (p_0, p_1, p_2); θ_1 is the angle of T_1 at p_1; p_2 and p_4 are passing points while the rest are turning points; the dotted path $p_0 \to p_1 \to p_2$ is P_1; the complement path denoted by the set of solid line segments is $\bar{P}_1$; $\mathcal{U}_1 = \{U_1, U_2\}$ is the set of active neighborhoods at p_1. Notice that the binding neighborhood U_3 is not active since it intersects $\bar{P}_1$.

3.1 Neighborhood-Related Objects

By our previous discussion, any optimal solution of TSPN must be a Hamiltonian tour $(p_0, \mathbf{p})$ for some $\mathbf{p} \in \prod_{i \in I} U_i$. One caveat of this representation is that it might contain repeated points, since the neighborhoods can overlap. Therefore, multiple visits to different neighborhoods may occur at the same location. To remove the symmetries that may arise from such repetitions, we instead use a reduced representation $(p_k)_{k=0}^K$ that contains only distinct points. This represents the closed tour with the shortest distance that starts at p_0, then travels between each pair of consecutive points p_k and p_{k+1} , before returning to p_0. This point sequence representation is quite natural to the problem setting and has been commonly used in the TSPN and CETSP literature (Arkin and Hassin, 1994, Behdani and Smith, 2014, Coutinho et al., 2016, Carrabs et al., 2017). For each point p_k, we also define $\hat{\mathcal{U}}_k := \{U_i \in \mathcal{U} \mid p_k \in U_i\}$ to be the set of *binding neighborhoods* at p_k. A sequence $(p_k)_{k=0}^K$ is feasible if $\{\hat{\mathcal{U}}_k\}_{k=0}^K$ is a nonempty cover of $\mathcal{U}$, i.e., $\hat{\mathcal{U}}_k \neq \varnothing$ for all k and their union is $\mathcal{U}$. A sequence is then said to be optimal if it has the shortest length among all feasible sequences.

Definition 3. *Given a feasible sequence $\gamma = (p_k)_{k=0}^K$, we define the following associated objects:*

- *T_k is the convex combination of points $\{p_{k-1}, p_k, p_{k+1}\}$;*
- *$\theta_k \in [0, \pi]$ is the angle of T_k at the point p_k;*
- *p_k is called a* passing point *if $\theta_k = \pi$, and a* turning point *otherwise;*
- *P_k is the path $p_{k-1} \to p_k \to p_{k+1}$;*
- *$\bar{P}_k$ is the complement path of P_k in the closed tour γ, i.e.,*

$$\bar{P}_k = p_{k+1} \to p_{k+2} \to \cdots \to p_0 \to p_1 \to \cdots \to p_{k-1}$$

- *$\mathcal{U}_k := \{U_i \in \hat{\mathcal{U}}_k \mid U_i \cap \bar{P}_k = \varnothing\}$ is called the set of* active neighborhoods *at p_k.*

The following lemma reveals an interesting relationship between a turning point p_k and its active neighborhoods.

Lemma 1. *If the point p_k is a turning point in an optimal sequence γ^*, then the set of active neighborhoods $\mathcal{U}_k$ is nonempty.*

Also, the next lemma will be used in the following sections. It can be trivially proven by sequentially applying the triangle inequality (see Figure 5), so we omit the proof.

Lemma 2. *For any triangle $T = (a, b, c)$ where a, b, c are three points in $\mathbb{R}^2$ such that the angle at b is within the interval $[0, \pi)$, let b' be any point in T such that $b' \neq b$; then we have,*

$$\delta(a, b) + \delta(b, c) > \delta(a, b') + \delta(b', c).$$

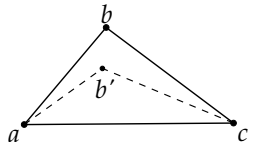

Figure 5: Illustration of Lemma 2.

3.2 Local conditions

When solving TSPN, Behdani and Smith (2014) proved that any optimal TSPN tour can be represented by an ordered set of turning points, each of which is located on the boundary of some neighborhood. In this section, we strengthen this conclusion by analyzing the relation between the objects associated with each turning point p_k. The main theorem follows.

Theorem 1. *If p_k is a turning point in an optimal sequence γ^*, then there must exist a neighborhood $U_i \in \mathcal{U}_k$ such that $U_i \cap P_k = \{p_k\}$. Moreover, if all neighborhoods in $\mathcal{U}_k$ are also path-connected, then there is some $U_i \in \mathcal{U}_k$ such that $U_i \cap T_k = \{p_k\}$.*

Notice that both $U_i \cap P_k = \{p_k\}$ and $U_i \cap T_k = \{p_k\}$ imply that $\{p_k\}$ is on the boundary of U_i. Thus, this theorem establishes a stronger optimality criterion than the one in Behdani and Smith (2014) by using the relation between some active binding neighborhood $U_i \in \mathcal{U}_k$ and the associated path P_k or triangle T_k. The extra path-connectedness requirement in the second statement of Theorem 1 is necessary due to the possibility that multiple neighborhoods may be binding at the same turning point. If all neighborhoods are known to be disjoint, the following corollary provides a similar result without requiring path-connectedness.

Corollary 1. *Let p_k be any turning point of an optimal sequence γ^* and $\mathcal{U}_k$ be the associated active neighborhoods. If all neighborhoods in $\mathcal{U}_k$ are disjoint, then the unique choice $U_i \in \mathcal{U}_k$ satisfies $U_i \cap T_k = \{p_k\}$ for all k.*

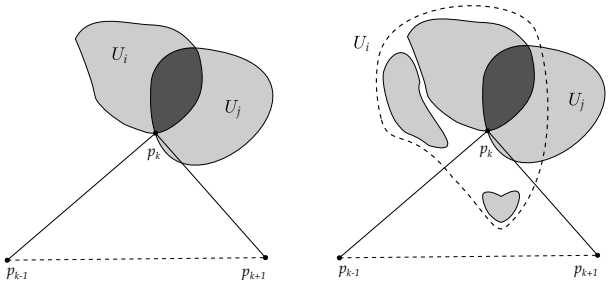

Figure 6: Illustration of the local optimality criteria for path-connected and path-disconnected neighborhoods.

Both Theorem 1 and Corollary 1 give local conditions associated with each of the turning points in an optimal sequence γ^*. Thus, we call them the local conditions. Furthermore, the proofs of both statements essentially provide constructive procedures to produce a strictly shorter feasible sequence from a given sequence that violates this criteria. Therefore, these results can be utilized to generate better feasible sequences in subroutines of various TSPN algorithms.

3.3 Global Conditions

The local conditions derived previously describe the relation between each turning point p_k of an optimal TSPN tour γ^* and the associated path P_k or triangle T_k. In contrast, the global conditions that will be presented in this section characterize the location of the entire optimal tour γ^*. Assuming that all neighborhoods are disks, Behdani and Smith (2014) have shown that the optimal tour γ^* must lie within the convex hull induced by all the centers of the disks. In this subsection, we generalize this result to compact neighborhoods with arbitrary shapes. We will focus only on neighborhoods in the two-dimensional Euclidean space, but most results can be easily extended to higher dimensions.

We start with some notation. Let ∂U be the boundary of U (i.e., the closure of U without its interior under Euclidean topology). In particular, for some half-plane $H = \{x \in \mathbb{R}^2 \mid a^T x \leq b\}$, the boundary ∂H is the straight line $\{x \in \mathbb{R}^2 \mid a^T x = b\}$. For a half-plane $H \subseteq \mathbb{R}^2$ and a point $x \in \mathbb{R}^2$, we use $\text{proj}_H(x)$ to denote the projection of x onto the straight line ∂H. Then, we define the following.

Definition 4. *Given a compact neighborhood U and a half-plane H, U is* boundary-projection-closed *(BPC) with respect to H if for every point $x \in \partial U \setminus H$, $proj_H(x) \in U$. We call this half-plane H a BPC separator of U. Similarly, given a set of neighborhoods $\mathcal{U}$, a half-plane H is a BPC separator of $\mathcal{U}$ if it is a BPC separator of every U in $\mathcal{U}$. We denote $\mathcal{H}_\mathcal{U}$ the set of all BPC separators of $\mathcal{U}$.*

This definition uses a set of compact neighborhoods $\mathcal{U}$ to characterize a certain type of half-plane. Figure 7(a) provides an example. By definition, both half-planes H_1 and H_3 are BPC separators, but H_2 is not because the projection of some boundary point is not contained in the same neighborhood. Notice that, for any family of compact neighborhoods $\mathcal{U}$, $\mathcal{H}_\mathcal{U}$ is nonempty as any half-plane that contains all the neighborhoods in $\mathcal{U}$ is trivially a BPC separator of $\mathcal{U}$ (e.g., half-plane H_3).

Given a fixed visiting order σ, we use γ^*_σ to denote a local optimal TSPN tour that conforms to the visiting order σ. Then, the next theorem describes the relation between a BPC separator H and any local optimal TSPN solution γ^*_σ. We first introduce the following definition.

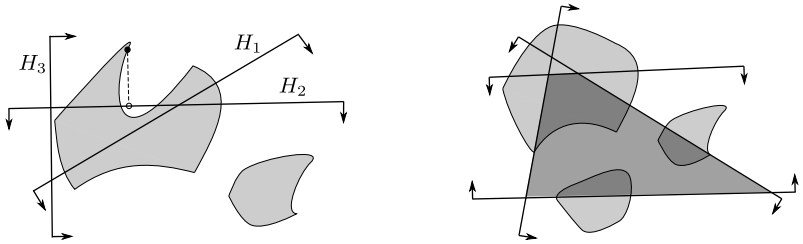

(a) (b)

Figure 7: Illustration of projection-closed separators.

Definition 5 (Redundant Tours)**.** *Given a set of neighborhoods $\mathcal{U}$ and a BPC separator H of $\mathcal{U}$, we say a feasible tour γ is redundant relative to H if $\gamma \cap H = \varnothing$ and γ lies in a straight line that is parallel to ∂H. We say γ is non-redundant if it is not redundant relative to any BPC separator H.*

By this definition, a redundant tour relative to H is a feasible tour outside H that is parallel to the boundary ∂H. Thus, it has the property that its projection onto ∂H forms a non-redundant tour with the same length. Moreover, this non-redundant tour is still feasible as H is a BPC separator.

Theorem 2. *Given a set of neighborhoods $\mathcal{U}$, a BPC separator H of $\mathcal{U}$, and a visiting sequence σ, every non-redundant local optimal tour γ_σ^* is inside the half-plane H.*

One implication of Theorem 2 is that every non-redundant local optimal tour lies inside the intersection of any family of BPC separators of $\mathcal{U}$. For instance, in Figure 7(b), any local optimal tour cannot lie in a straight line. Thus, it is in the convex hull enclosed by the BPC separators. We define *domination hull* as the smallest intersection containing all the non-redundant local optimal tours.

Definition 6 (Domination Hull)**.** *Given a set of compact neighborhoods $\mathcal{U} = \{U_i\}_{i\in I_0}$, we define the following recursive construction procedure, where $k \in \mathbb{N}$ is the given iteration,*

1. *Step 1: initially, let $U_i^0 = U_i$ for all $i \in I_0$;*
2. *Step 2: $\mathcal{U}_k = \{U_i^k\}_{i\in I_0}$;*
3. *Step 3: $D_{\mathcal{U}_k} = \bigcap \mathcal{H}_{\mathcal{U}_k}$, where $\mathcal{H}_{\mathcal{U}_k}$ contains all the BPC separators of the neighborhoods $\mathcal{U}_k$;*
4. *Step 4: $U_i^{k+1} = U_i^k \cap D_{\mathcal{U}_k}$ for all $i \in I_0$. Go to Step 2.*

Then, the domination hull $D_{\mathcal{U}}$ is defined as the limit of $D_{\mathcal{U}_k}$, i.e., $D_{\mathcal{U}} = \lim_{k\to\infty} D_{\mathcal{U}_k}$.

Essentially, the domination hull $D_{\mathcal{U}}$ is obtained by sequentially reducing all the neighborhoods using all the available BPC separators until no further reduction can be made. The reason for multiple iterations is that new BPC separators may emerge after each intersection operation (see Figure 8).

The following corollary characterizes the domination hull $D_{\mathcal{U}}$ for any neighborhood set $\mathcal{U}$.

Corollary 2. *Given a set of compact neighborhoods $\mathcal{U}$, if the optimal tour γ^* does not lie in a straight line, then the domination hull $D_{\mathcal{U}}$ is a nonempty, convex, compact set.*

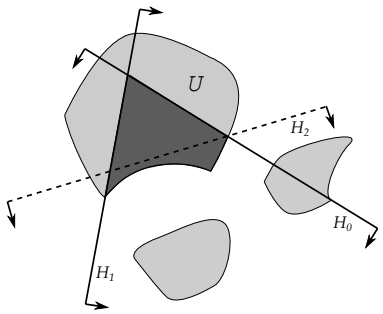

Figure 8: A new BPC separator H_2 that emerges after adding the two separators H_0 and H_1.

3.3.1 Domination Hull Approximation.

In general, constructing the exact domination hull is a non-trivial task, as it may require an infinite number of iterations of the procedure given in Definition 6 to fully converge. However, we can approximate it by stopping this procedure at any time we choose as long as a bounded polygon $D'_{\mathcal{U}}$ is obtained. Then, all the non-redundant local optimal tours, including the global optimal solution, are still inside $D'_{\mathcal{U}}$ according to Theorem 2.

Algorithm 1 presents a pseudocode for constructing an approximation of the domination hull. This algorithm requires some preprocessing steps. First, we compute a sufficiently small circle centered at O with a radius r that circumscribes all the neighborhoods in $\mathcal{U}$ where O is the origin of the plane. Then, for a given angle $\theta \in [0, 2\pi)$ and a distance d, we use $H_{\theta,d}$ to denote the unique half-plane that satisfies: (1) $O \in H_{\theta,d}$, (2) the angle between the line segment $[O, \text{proj}_{H_{\theta,d}}(O)]$ and the x-axis is θ, and (3) the length $\delta(O, \text{proj}_{H_{\theta,d}}(O))$ is d.

Algorithm 1: Domination Hull Approximation

input : a set of neighborhoods $\mathcal{U}$
output: a set of BPC separators

set the number of iterations N;
$\mathcal{H} \leftarrow \varnothing$; `// the set of BPC separators`
for $i \in N$ **do**
  $\theta \leftarrow 2\pi(i-1)/N$;
  $d \leftarrow$ `BinarySearch(0, r, θ, U)` ; `// search for` d `such that` $H_{\theta,d} \in \mathcal{H}_{\mathcal{U}}$
  $\mathcal{H} \leftarrow \mathcal{H} \cup \{H_{\theta,d}\}$;
  $\mathcal{U} \leftarrow \{U \cap H_{\theta,d} \mid U \in \mathcal{U}\}$; `// reduce the neighborhoods by the new separator` $H_{\theta,d}$
end
return $\mathcal{H}$;

At each iteration, this algorithm first enumerates an angle θ. There are many angle enumeration schemes that can be used, such as an equiangular enumeration, a random enumeration, or an angle bisection. For the following demonstration, we choose the equiangular enumeration scheme described in Algorithm 1. For every enumerated angle θ, the algorithm generates a BPC separator $H_{\theta,d}$ where the distance d is returned by the binary search subroutine provided in Algorithm 2. To run this subroutine, a BPC separator verifier is required. The implementation of this verifier also depends on the specific neighborhood representations. For instance, if each neighborhood is the intersection of half-planes or a sequence of points, then verifying

Algorithm 2: Binary Search

input : a, b, θ, $\mathcal{U}$
output: a distance scalar

set a small value $\epsilon > 0$;
if $b - a \leq \epsilon$ **then**
  return b;
end
$c \leftarrow (a + b)/2$;
if `BPCVerify`($H_{\theta,c}$, $\mathcal{U}$) *is* **true then**
  return `BinarySearch`(a, c, θ, $\mathcal{U}$);
else
  return `BinarySearch`(c, b, θ, $\mathcal{U}$);
end

the turning points on the boundary is sufficient; if the neighborhoods are ellipsoids, we can even replace the binary search subroutine by finding the two tangent lines of every ellipsoid that are perpendicular to $H_{\theta,c}$. After generating a new half-plane $H_{\theta,d}$, the last step in the for-loop is to trim each neighborhood by the newly generated $H_{\theta,d}$.

In general, the binary search subroutine only returns a locally minimized distance d. However, based on Proposition 2, it converges to the global minimum when all neighborhoods are convex.

Proposition 2. *Given a set of convex neighborhoods $\mathcal{U}$, the binary search subroutine described in Algorithm 2 converges to the minimized distance*

$$\begin{aligned} &\min\ d \\ &s.t.\ H_{\theta,d} \in \mathcal{H}_{\mathcal{U}}, \\ &\quad d \in [0, r], \end{aligned}$$

when $\epsilon \to 0$.

Note that, if all neighborhoods are convex, the trimming operation in the last step of the for-loop in Algorithm 1 preserves convexity. Thus, intuitively, when N and ϵ converge to ∞ and 0, the intersection of the BPC separators $\mathcal{H}$ returned by Algorithm 1 converges to the domination hull $D_{\mathcal{U}}$.

In the next section, we will propose a mixed-integer nonlinear programming model for solving PDTSPN with convex neighborhoods. The BPC separators can be generated as a pre-processing step to cut off some portions of the neighborhoods that contain suboptimal visiting points, which may significantly reduce the overall solution space.

4 Mathematical Formulation for PDTSPN

In the previous section, we proposed two optimality conditions for TSPN that are valid for neighborhoods with general geometric properties. As discussed before, the inner problem of Formulation (1) can be strengthened by using these results. In this section, we focus on PDTSPN, and provide a mathematical formulation along with a solution approach.

For this formulation, we use binary variables $u = \{u_{ij} \mid i, j \in I_0 \text{ and } i \neq j\}$ to indicate whether

neighborhood U_i appears immediately before neighborhood U_j in the optimal tour, and use z_{ij} to represent the distance between the two points $(x_i, y_i) \in U_i$ and $(x_j, y_j) \in U_j$, where the visits to such neighborhoods take place. Given any visiting sequence $\sigma \in S_n$ that violates the supply and demand requirements given by constraints (1b), let $k \in I$ be the first neighborhood in σ that violates the corresponding constraint (1b) and denote $T = \{(i-1, i)\}_{i=1}^{k}$ the violating subpath of σ. Furthermore, let $\mathcal{T}$ comprise the set of violating subpaths associated with all the infeasible visiting sequences in S_n. Then, Formulation (1) admits the following nonlinear program,

$$\min \quad \sum_{i,j \in I_0, i \neq j} u_{ij} z_{ij} \tag{3a}$$

$$\text{s.t.} \quad \sum_{j \in I_0, j \neq i} u_{ij} = 1, \qquad \forall\, i \in I_0, \tag{3b}$$

$$\sum_{j \in I_0, j \neq i} u_{ji} = 1, \qquad \forall\, i \in I_0, \tag{3c}$$

$$\sum_{i,j \in I', i \neq j} u_{ij} \leq |I'| - 1, \qquad \forall\, I' \subsetneq I_0, |I'| \geq 2, \tag{3d}$$

$$\sum_{(i,j) \in T} u_{ij} \leq |T| - 1, \qquad \forall\, T \in \mathcal{T}, \tag{3e}$$

$$f_i(x_i, y_i) \leq 0, \qquad \forall\, i \in I, \tag{3f}$$

$$(x_i - x_j)^2 + (y_i - y_j)^2 \leq z_{ij}^2, \qquad \forall\, i, j \in I_0, i \neq j, \tag{3g}$$

$$x_i, y_i \text{ free}, \qquad \forall\, i \in I_0, \tag{3h}$$

$$z_{ij} \geq 0, \qquad \forall\, i, j \in I_0, i \neq j \tag{3i}$$

$$u_{ij} \in \{0, 1\}, \qquad \forall\, i, j \in I_0, i \neq j. \tag{3j}$$

The objective function (3a) minimizes the traveling distance of the tour. Constraints (3b)–(3d) and (3j) are adapted from the Danzig–Fulkerson–Johnson (DFJ) formulation for TSP that ensures every feasible solution is a Hamiltonian tour over I_0. Constraint (3e), which is equivalent to Constraint (1b), eliminates all the visiting sequences starting at the depot that violate the supply and demand requirements. Constraint set (3f) represents the neighborhoods. Finally, (3g)–(3i) indicate that z_{ij} is the Euclidean distance between the points (x_i, y_i) and (x_j, y_j).

4.1 Solution Approach

Let E_{sd} and $\bar{E}_{sd}$ be the set of solutions that satisfy (3b)–(3e) with and without constraint set (3j), respectively. That is, $\bar{E}_{sd}$ is a polyhedron obtained by relaxing the binary constraints of E_{sd}. Then, we define $\Phi(u)$ as follows.

$$\Phi(u) := \min_{x,y,z} \left\{ \sum_{i,j \in I_0} u_{ij}(z_{ij} - \bar{z}_{ij}) \mid \text{ Constraints (3f)–(3i)} \right\}, \tag{4}$$

where $\bar{z}_{ij}$ is the minimum distance between neighborhoods U_i and U_j defined as

$$\bar{z}_{ij} := \min_{x_i \in U_i, x_j \in U_j} \|x_i - x_j\|_2.$$

With these notations, Formulation (3) can be equivalently written as,

$$\min \quad \sum_{i,j \in I_0, i \neq j} \bar{z}_{ij} u_{ij} + \theta \tag{5a}$$

$$\text{s.t.} \quad u \in E_{sd}, \tag{5b}$$

$$\theta \geq \Phi(u), \tag{5c}$$

$$\theta \geq 0. \tag{5d}$$

Because $\bar{z}_{ij}$, by definition, is a valid lower bound of z_{ij} for all $i, j \in I_0$, this reformulation allows us to initialize the objective of any feasible solution u to be at least as large as the lower bound $\sum_{i,j \in I_0} \bar{z}_{ij} u_{ij}$. Another observation is that, when the neighborhood functions f's are convex, the subproblem $\Phi(u)$ belongs to the class of convex optimization. For instance, if the f's are either the intersection of half-planes or ellipsoids, $\Phi(u)$ is a second-order cone program. In this case, $\Phi(u)$ admits a dual representation that satisfies strong duality and can be solved efficiently. Moreover, the resulting problem can be solved via the generalized Benders decomposition (Geoffrion, 1972).

To this end, we decompose Formulation (3) into a master problem, obtained directly from Formulation (5) by replacing (5c) with a set of *generalized Benders optimality cuts* (GBCs), which are iteratively generated by the subproblem $\Phi(u)$ The outline of the algorithm is as follows. At each iteration, we solve the master problem under the current set of GBCs to obtain a candidate visiting order $u^* \in E_{sd}$ and an estimated value of θ^*. Then, we solve subproblem $\Phi(u)$ parameterized with such an order to find the optimal visiting points of the corresponding tour. Then, if the optimal value of the subproblem is larger than θ^*, we generate a new GBC and add it to the current constraint pool of the master problem.

By this design, at each iteration, the value of the master problem always serves as a lower bound, and the value that results by replacing θ^* with the optimal subproblem's objective is an upper bound as it finds the optimal visiting locations of the given feasible order. This iterative procedure terminates when a desired gap between the lower and upper bounds is achieved. In the next subsection, we will discuss the implementation details of the master problem and the subproblem.

4.2 Implementation Details

As with most Benders decomposition approaches, constraint (5c) in the master problem is replaced by a set of GBCs that are produced iteratively from the subproblem. Also, constraint (5b) is composed of constraints from (3b)–(3e) and (3j). In particular, since both the subtour elimination constraint set (3d) and the supply-demand constraint set (3e) are potentially quite large in practice, even for instances of moderate sizes, we employ an iterative separation method commonly used to handle such constraints (Behdani and Smith, 2014).

At each iteration, when solving the master problem, we use the following procedure to iteratively produce a feasible visiting order that satisfies the supply and demand constraints:

1. Initialize the master problem with a subset (possibly empty) of constraint sets (3d) and (3e);
2. Solve the master problem to obtain a candidate solution u^*;

3. Following the visiting order represented by u^*, test whether the supply-demand constraints (1b) are violated or whether u^* contains a subtour. This may result in the following three possible cases:

   (a) at a certain neighborhood $i \in I_0$, the corresponding subpath T associated with the visiting order violates the supply-demand requirements. In that case, we add the corresponding violated constraint (3e) into the master problem and then go back to Step 2;

   (b) the candidate solution contains a subtour, in which case we add the corresponding subtour elimination constraint (3d) into the master and then go back to Step 2;

   (c) otherwise, the subroutine returns a feasible visiting order.

For subproblem $\Phi(u)$ as long as functions f's are convex, $\Phi(u)$ is a convex optimization problem. Therefore, any off-the-shelf solver able to handle such type of problems can be used to obtain an optimal solution (x^*, y^*, z^*).

Let π^* and μ^* be the optimal value of the dual variables associated with constraints (3f) and (3g). Then, the GBCs, as given by Geoffrion (1972), are as follows:

$$\theta \geq \sum_{i,j \in I_0, i \neq j} u_{ij}(z^*_{ij} - \bar{z}_{ij}) - \sum_{i \in I_0} \pi^*_i f_i(x^*_i, y^*_i) - \sum_{i,j \in I_0, i \neq j} \mu^*_{ij}((x^*_i - x^*_j)^2 + (y^*_i - y^*_j)^2 - z^*_{ij}). \tag{6}$$

Furthermore, notice that since u only appears in the subproblem's objective and not in constraints (3f) and (3g), the last two terms in (6) can be omitted, as they are always equal to zero by complementary slackness. The GBCs can then be expressed as

$$\theta \geq \sum_{i,j \in I_0, i \neq j} u_{ij}(z^*_{ij} - \bar{z}_{ij}). \tag{7}$$

This is quite convenient in practice, as constraints (7) can be generated directly by solving the (primal) subproblem $\Phi(u)$ without the need for an optimal dual solution (π^*, μ^*). We note that the subproblem $\Phi(u)$ is feasible for any given visiting sequence produced by the master problem (3). Thus, our implementation does not require feasibility cuts. Furthermore, according to the following proposition, this cut generation approach is also exact for problems with non-convex neighborhoods.

Proposition 3. *Given non-convex region representations in* (3f)*, the cut generation implementation of* (5) *with GBCs from* (7) *solves for an optimal solution of* (3)*.*

In the following subsection, we introduce the specific non-convex neighborhood characterization of (3f) that will be used in our experiment.

4.3 Representation for Non-Convex Neighborhoods

There are multiple ways to describe non-convex neighborhoods in (3f). For instance, we can represent them using unions of convex neighborhoods or by discretizing the boundaries. The latter representation introduced and implemented in Behdani and Smith (2014) has several advantages: it does not require the neighborhoods to have closed-formed descriptions, and it can approximate most compact neighborhoods arbitrarily closely with a fine-tunable degree of granularity. In this subsection, we introduce a variant of such a characterization.

Given a neighborhood U_i, we use a finite sequence of points $(v_j)_{j\in[m]}$ with $[m] := \{1, 2, \ldots, m\}$ to represent the non-convex polygon approximation of U_i defined by the closed loop

$$v_1 \to v_2 \to \cdots \to v_m \to v_1,$$

and use $\iota(j)$ to denote the next index of j in a circular fashion, i.e., $\iota(j) = j + 1$ for $j < m$ and equals to 1 for $j = m$. Then, the boundary of this approximation of U_i can be described as follows,

$$(x, y) = \sum_{j\in[m]} \left(\phi_j \cdot \left(\lambda v_j + (1-\lambda)v_{\iota(j)}\right)\right), \tag{8a}$$

$$\sum_{j\in[m]} \phi_j = 1, \tag{8b}$$

$$\lambda \in [0, 1],\ \phi_j \in \{0, 1\},\ \forall j \in [m]. \tag{8c}$$

This model enforces that any point (x, y) in the boundary of this polygonal approximation of U_i is located in one of the line segments connecting two consecutive points in (v_j). The corresponding linearized version follows,

$$(x, y) = \sum_{j\in[m]} \left(\lambda_j \left(v_j - v_{\iota(j)}\right) + \phi_j v_{\iota(j)}\right), \tag{9a}$$

$$\sum_{j\in[m]} \phi_j = 1, \tag{9b}$$

$$\lambda_j \le \phi_j,\ \forall j \in [m], \tag{9c}$$

$$\lambda_j \ge 0, \phi_j \in \{0, 1\},\ \forall j \in [m]. \tag{9d}$$

By the local optimality criterion proven in Theorem 1, the turning points of an optimal solution lie on the boundary of the neighborhoods. Hence, combining this boundary representation for non-convex polygons and the cut generation implementation introduced in the last subsection, we have an exact solution approach for solving the PDTSPN problem with non-convex neighborhoods to any desired precision, based on the granularity of the polygonal approximation.

With a slight modification, this solution approach can also be adapted to solve PDTSPN with other supply-demand precedence relationships.

4.4 Solution Approaches for Modeling Other Supply-Demand Precedences

Up to this point, our discussion has been focused on the M-M version of the problem. Therefore, to solve any of the other variants described in Section 1, Formulation (3) must be adapted to represent the corresponding demand-supply precedence requirements. In general, under some minor considerations, this can often be done by simply identifying the corresponding set $\mathcal{T}$ of violating subpaths in constraints (3e). In this subsection, we illustrate how to do this for the 1-M-1 and the 1-1 versions.

4.4.1 1-M-1 PDTSPN.

For this case, given any visiting sequence $\sigma \in S_n$, one can check whether a vehicle following σ has sufficient capacity when visiting each supply neighborhood to satisfy the given pick up requirements. That is, for every node $i \in I_s$, one can test whether

$$s_0 + \sum_{j \le i:\sigma(j) \in I_s} s_j - \sum_{j \le i:\sigma(j) \in I_d} d_j \le c.$$

If such a condition is violated by σ at neighborhood k, then, the violating subpath $T = \{(i-1, i)\}_{i=1}^{k}$ exists in $\mathcal{T}$. As before, constraint set (3e) can also be populated iteratively via branch and cut.

4.4.2 1-1 PDTSPN.

For this case, it is possible to adapt the definition of set $\mathcal{T}$. Specifically, for the supply-demand neighborhood pair, denoted by (s_q, d_q), associated with some commodity q, one simply needs to add to $\mathcal{T}$ all the subpaths in which s_q appears before d_q. Alternatively, we now show that it is possible to impose such precedence requirements by adding instead a set of constraints of size polynomial, which has the benefit of not requiring the iterative separation process of constraints (3e). We now provide two possible ways of modeling these requirements.

In the first method, we add artificial binary variables $g = \{g_{ij} \mid i, j \in I_0 \text{ and } i \neq j\}$ into the formulation to explicitly indicate whether neighborhood i appears before j in the visiting sequence. Then, the following constraints along with (5b) enforce the desired precedence requirement.

$$u_{ij} \le g_{ij}, \quad \forall\, i, j \in I_0 \tag{10a}$$

$$u_{ik} + u_{kj} - 1 \le g_{ij}, \quad \forall\, k \in I \setminus \{i, j\} \tag{10b}$$

$$g_{ji} = 0, \quad \text{for all supply-demand pairs } (i, j). \tag{10c}$$

Another possible way to model the precedence requirement is using the flow constraints introduced in Hernández-Pérez and Salazar-González (2009). The basic idea is that under (5b), a positive flow from i to j ensures that $u_{ij} = 1$ and $u_{ji} = 0$. Specifically, for each supply-demand pair, denoted by (s_q, d_q), we need to transfer a unit of commodity q from s_q to d_q. Let $r_{ij}^q \in [0, 1]$ be the flow of commodity q between consecutive neighborhoods i and j, then we have the following set of constraints to impose the required precedence relation. Note that, because of Assumption 1(*ii*), the commodity flow between each supply-demand neighborhood pair can be capped at one unit w.l.o.g.

$$r_{ij}^q \le u_{ij}, \quad \forall\, i, j \in I_0, k \in K, \tag{11a}$$

$$\sum_{j \in I_0} r_{ji}^q - \sum_{j \in I_0} r_{ij}^q = \begin{cases} 1, & \text{if } i = s_q, \\ -1, & \text{if } i = d_q, \\ 0, & \text{otherwise,} \end{cases} \quad \forall\, i \in I, q \in Q. \tag{11b}$$

For many other PDTSPN variants, similar strategies can be adopted to modify Formulation (3) and its implementation.

5 Numerical Experiments

In this section, we conduct computational experiments to test the different developments presented in this work. We focus on two types of problems: (i) instances with only convex neighborhoods and (ii) instances with both convex and non-convex neighborhoods. For (i), we analyze the effectiveness of the proposed domination hull algorithm (Algorithm 1) in terms of the size reduction of the neighborhoods and test the performance of the generalized Benders decomposition method with respect to the solution times, optimality gaps, and cut separation times. To demonstrate the flexibility of this solution approach, we perform our algorithm on instances with two types of supply-demand precedence relationships, namely 1-1 and M-M. For (ii), we are interested in the performance of the non-convex representation (9), the runtime efficiency enhanced by the domination hull algorithm, and the impact of neighborhoods' location in the area under consideration (see Figure 10).

We conducted our experiments on a computer equipped with an Intel(R) Core(TM) i7-11700F 2.50GHz processor and 16GB of RAM and running Windows 10. All the algorithms were implemented in Python 3.6.9 and solved by the commercial optimizer Gurobi 9.1.2 with a one-hour time limit.

5.1 Experiments with Convex Neighborhoods

5.1.1 Test Instances.

We generate 195 instances with different numbers and sizes of neighborhoods, where n, the number of neighborhoods, ranges from $\{6, 8, \ldots, 30\}$. All neighborhoods of each instance are assumed to be convex polygons generated from 10 randomly chosen points within a ℓ by ℓ square, where the side length $\ell \in \{0.75, 1, 1.25\}$ controls the upper limit of the neighborhood size. We call this length ℓ the size controller hereafter. To locate these neighborhoods, the center (x, y) of every square (as well as the depot) are randomly picked from intervals $[0, 16]$ and $[0, 10]$.

For each 1-1 PDTSPN instance, we generated the supply-demand pairs by randomly pairing two numbers from the index set $I = \{1, 2, \ldots, n\}$. For each M-M PDTSPN instance, the supply or demand quantity of each neighborhood is a positive integer randomly generated from $\{1, 2, \ldots, 10\}$. We also ensure that the sums of supplies and demands are equal.

Under these settings, it should be clear that the complexity of an instance mainly depends on the number of neighborhoods n and the size controller ℓ, since all the other parameters are either identical or random. Therefore, we call every pair (n, ℓ) an instance configuration. For both the 1-1 and M-M versions, we generate five instances for each configuration. In the following tables, we aggregate the computational results for each instance configuration and present the averages, as instances with the same configuration are expected to yield similar results.

5.1.2 Domination Hull Approximation.

In this experiment we assume all regions are convex; therefore, the subproblem $\Phi(u)$ of the proposed Benders decomposition approach is a second-order cone program, which can be solved quite efficiently for any given u. Hence, it is expected that BPC separators and the corresponding domination hull will have a lesser impact on the runtime performance of the algorithm. Nevertheless, we report here the size reduction of the neighborhoods resulting from the domination hull approximation algorithm (Algorithm 1) since it shows

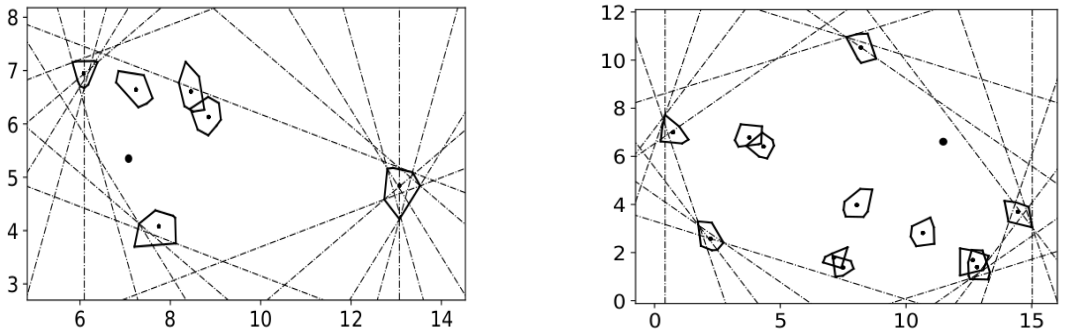

(a) The number of neighborhoods $n = 6$ (b) The number of neighborhoods $n = 12$

Figure 9: Illustration of separators (dashed lines) generated by Algorithm 1

some interesting relationship between the instance configurations and the size reduction effectiveness. For problems with more difficult subproblems, such as instances with non-convex neighborhoods in Section 5.2, this effectiveness in size reduction will eventually translate into runtime efficiency.

To study the performance of Algorithm 1, for each configuration, we generate 10, 16, 22, and 28 separators and report the corresponding neighborhood size, the size reduction in percentage, and the runtime in seconds in Table 1.

In general, Algorithm 1 seems to be quite efficient at identifying domination hull approximations. It halts within a second on all the test instances thanks to the binary search implementation. As expected, the running times increase as the number of separators and neighborhoods increase.

The results in Table 1, show the average percentage of the area that is cut off by the BPC separators. We observe that a sizable portion of the neighborhood area, ranging from 7% to 47%, is trimmed by the separators in each instance. This phenomenon is more significant for instances with a smaller n. For instance, when $n = 6$, an average of 31.66% of the neighborhood area is removed by merely 10 separators, and this number increases to 45.96% with 28 generated separators. They are significantly larger than the corresponding numbers 8.47% and 12.74% in the case $n = 30$. The reason is that the domination hull is essentially determined by the peripheral neighborhoods (see Figure 9). When more neighborhoods are present, more of them are likely to lie in the interior of the domination hull. For instance, in Figure 9(a), only two out of six neighborhoods are not affected by the separators, while five out of twelve neighborhoods are not affected in Figure 9(b).

Another interesting observation is that the law of diminishing marginal utility seems to apply on the trimming effects of the separators. In Table 1 can be observed that, for every configuration, the compound area reduction diminishes as the number of separators increases. This phenomenon suggests that one can set the implementation to stop after a small set of separators are added to save computational resources without compromising much on the quality of the separators.

5.1.3 Generalized Benders Decomposition Approach.

In this part, we analyze the computational results of the generalized Benders decomposition approach introduced in Section 4.

For each configuration, we aggregate and report the numbers of subtour elimination cuts, supply-demand

Table 1: Results for the domination hull approximation algorithm (Algorithm 1). For each configuration, we generate 10, 16, 22, and 28 separators and report the corresponding neighborhood size (Area Size), the size reduction in percentage (Cutoff Pct (%)), and the runtime in seconds (Time)

		10 Separators		16 Separators		22 Separators		28 Separators	
n	l	Cutoff Pct (%)	Time	Cutoff Pct (%)	Time	Cutoff Pct (%)	Time	Cutoff Pct (%)	Time
6	0.75	36.30	0.08	39.63	0.11	42.15	0.16	45.20	0.20
	1	30.40	0.08	36.01	0.14	41.96	0.18	46.58	0.23
	1.25	28.29	0.08	34.97	0.12	40.92	0.17	46.09	0.22
	Avg	31.66	0.08	36.87	0.13	41.68	0.17	45.96	0.22
8	0.75	20.97	0.10	29.56	0.16	32.48	0.22	35.50	0.28
	1	23.20	0.11	27.39	0.17	29.54	0.24	32.74	0.30
	1.25	26.89	0.11	28.91	0.17	33.43	0.24	34.96	0.30
	Avg	23.69	0.11	28.62	0.17	31.82	0.23	34.40	0.29
10	0.75	19.44	0.12	21.38	0.19	24.81	0.26	25.05	0.34
	1	18.84	0.12	19.36	0.19	22.66	0.26	23.94	0.33
	1.25	24.08	0.14	28.03	0.21	31.69	0.30	33.38	0.37
	Avg	20.79	0.13	22.92	0.20	26.39	0.27	27.46	0.35
12	0.75	17.75	0.16	20.01	0.24	24.16	0.33	26.50	0.42
	1	18.51	0.16	20.06	0.26	22.93	0.35	24.41	0.44
	1.25	18.55	0.13	21.13	0.21	23.36	0.29	26.29	0.37
	Avg	18.27	0.15	20.40	0.24	23.48	0.32	25.73	0.41
14	0.75	14.40	0.18	17.58	0.28	19.15	0.38	20.40	0.49
	1	17.06	0.19	20.43	0.30	24.10	0.41	24.35	0.52
	1.25	17.72	0.19	19.71	0.30	24.48	0.41	25.31	0.53
	Avg	16.40	0.19	19.24	0.29	22.58	0.40	23.35	0.51
16	0.75	13.09	0.19	17.20	0.31	18.45	0.43	19.31	0.55
	1	12.54	0.19	15.00	0.31	17.23	0.42	18.37	0.54
	1.25	12.08	0.19	14.28	0.31	17.12	0.42	18.05	0.54
	Avg	12.57	0.19	15.49	0.31	17.60	0.43	18.58	0.54
18	0.75	10.17	0.21	16.55	0.34	16.75	0.46	18.52	0.58
	1	11.37	0.21	13.50	0.35	16.30	0.47	16.13	0.60
	1.25	11.78	0.22	15.69	0.35	15.37	0.48	17.73	0.61
	Avg	11.11	0.21	15.25	0.34	16.14	0.47	17.46	0.60
20	0.75	10.58	0.23	11.82	0.35	14.11	0.49	14.33	0.62
	1	10.60	0.23	13.46	0.37	14.98	0.50	16.85	0.65
	1.25	11.09	0.22	13.72	0.36	15.77	0.50	16.56	0.65
	Avg	10.76	0.23	13.00	0.36	14.95	0.50	15.92	0.64
22	0.75	12.27	0.26	13.27	0.42	15.72	0.59	15.78	0.74
	1	10.70	0.28	13.05	0.44	14.71	0.60	15.98	0.77
	1.25	11.84	0.27	14.83	0.44	16.95	0.61	19.09	0.77
	Avg	11.60	0.27	13.72	0.44	15.79	0.60	16.95	0.76
24	0.75	9.58	0.30	11.49	0.47	12.52	0.65	12.85	0.83
	1	11.09	0.31	12.84	0.50	14.96	0.69	15.82	0.86
	1.25	9.12	0.27	12.17	0.44	13.90	0.62	14.21	0.77
	Avg	9.93	0.29	12.17	0.47	13.79	0.65	14.29	0.82
26	0.75	9.15	0.33	10.50	0.53	11.97	0.71	12.08	0.89
	1	8.09	0.28	11.43	0.45	12.30	0.64	13.44	0.80
	1.25	7.25	0.30	11.05	0.49	11.09	0.67	11.45	0.83
	Avg	8.17	0.30	10.99	0.49	11.79	0.67	12.32	0.84
28	0.75	8.28	0.32	10.97	0.52	12.24	0.71	13.60	0.90
	1	8.75	0.32	9.62	0.52	11.15	0.70	12.28	0.90
	1.25	8.65	0.31	10.86	0.50	11.63	0.67	12.26	0.86
	Avg	8.56	0.32	10.48	0.51	11.67	0.70	12.71	0.89
30	0.75	7.76	0.36	9.06	0.59	11.83	0.80	11.97	1.03
	1	8.84	0.38	10.63	0.60	11.60	0.83	12.67	1.04
	1.25	8.82	0.37	10.97	0.57	12.22	0.81	13.58	1.02
	Avg	8.47	0.37	10.22	0.59	11.88	0.81	12.74	1.03

Table 2: Results for the generalized Benders decomposition approach on 1-1 PDTSPN instances. For each configuration, we report the average number and separation time of subtour elimination cuts (Num. SECs and SEC Time), the average number and separation time of generalized Benders optimality cuts (Num. GBCs and GBC Time), the average total runtime for solving the instance (Model Time), the average optimality gap (MIP Gap), and the average percentage of instances solved to optimality (Opt. Pct).

n	l	Num. SECs	Num. GBCs	SEC Time	GBC Time	Model Time	MIP Gap (%)	Opt. Pct (%)
6	0.75	4.8	5.8	<0.001	0.058	0.078	0.00	100
	1	6.4	12.0	<0.001	0.116	0.147	0.00	100
	1.25	6.4	9.0	<0.001	0.085	0.102	0.00	100
	Avg	5.9	8.9	<0.001	0.086	0.109	0.00	100
8	0.75	15.2	14.8	<0.001	0.233	0.301	0.00	100
	1	8.0	13.6	<0.001	0.213	0.254	0.00	100
	1.25	10.8	11.0	<0.001	0.162	0.215	0.00	100
	Avg	11.3	13.1	<0.001	0.203	0.257	0.00	100
10	0.75	22.4	27.2	<0.001	0.622	0.737	0.00	100
	1	18.4	20.6	<0.001	0.457	0.559	0.00	100
	1.25	16.4	12.6	<0.001	0.281	0.404	0.00	100
	Avg	19.1	20.1	<0.001	0.454	0.567	0.00	100
12	0.75	34.0	27.8	<0.001	0.948	1.367	0.00	100
	1	13.2	19.6	<0.001	0.572	0.763	0.00	100
	1.25	52.8	45.8	0.001	1.384	1.716	0.00	100
	Avg	33.3	31.1	0.000	0.968	1.282	0.00	100
14	0.75	85.6	38.2	0.001	1.778	2.581	0.00	100
	1	90.0	41.0	0.001	1.788	2.639	0.00	100
	1.25	54.0	91.4	0.001	4.274	5.910	0.00	100
	Avg	76.5	56.9	0.001	2.613	3.710	0.00	100
16	0.75	72.4	66.6	0.001	3.457	5.969	0.00	100
	1	116.8	113.4	0.002	6.452	12.932	0.00	100
	1.25	95.6	363.8	0.002	20.200	27.446	0.00	100
	Avg	94.9	181.3	0.002	10.036	15.449	0.00	100
18	0.75	152.4	131.2	0.004	11.300	33.563	0.00	100
	1	423.6	124.4	0.017	10.698	390.422	0.00	100
	1.25	382.0	247.0	0.009	20.361	44.748	0.00	100
	Avg	319.3	167.5	0.010	14.119	156.245	0.00	100
20	0.75	190.4	164.6	0.005	18.292	116.984	0.00	100
	1	401.6	508.6	0.013	57.358	381.838	0.00	100
	1.25	402.4	542.6	0.014	61.908	637.254	0.00	100
	Avg	331.5	405.3	0.011	45.853	378.692	0.00	100
22	0.75	278.8	230.2	0.010	28.158	830.674	0.57	80
	1	830.0	471.2	0.044	58.693	2577.876	4.62	40
	1.25	592.0	492.0	0.030	62.129	1531.215	1.93	80
	Avg	566.9	397.8	0.028	49.660	1646.588	2.37	67
24	0.75	567.6	349.0	0.061	53.804	2305.244	2.96	60
	1	683.6	386.8	0.062	60.529	3118.071	10.16	20
	1.25	1096.4	880.2	0.137	138.192	3600.000	14.83	0
	Avg	782.5	538.7	0.087	84.175	3007.835	9.31	27
26	0.75	243.6	273.8	0.029	50.868	1576.985	1.87	80
	1	443.6	943.0	0.051	166.494	2853.801	1.21	80
	1.25	654.0	584.2	0.074	109.588	3600.000	14.47	0
	Avg	447.1	600.3	0.051	108.984	2676.984	5.85	53
28	0.75	322.4	358.2	0.023	73.885	3600.000	9.36	0
	1	588.4	377.2	0.072	80.385	3600.000	15.33	0
	1.25	1091.2	468.0	0.164	102.690	3600.000	22.59	0
	Avg	667.3	401.1	0.086	85.654	3600.000	15.76	0
30	0.75	790.8	334.4	0.130	85.099	3600.000	23.92	0
	1	474.4	513.0	0.041	129.715	3600.000	19.75	0
	1.25	430.8	521.0	0.058	155.943	3600.000	27.81	0
	Avg	565.3	456.1	0.077	123.586	3600.000	23.83	0

Table 3: Results for the generalized Benders decomposition approach on M-M PDTSPN instances. For each configuration, we report the average number and separation time of subtour elimination cuts (Num. SECs), supply-demand cuts (Num. SDCs), and generalized Benders optimality cuts (Num. GBCs). We also report the average model runtime (Model Time), the average optimality gap (MIP Gap), and the average percentage of instances solved to optimality (Opt. Pct).

n	l	Num. SECs	Num. SDCs	Num. GBCs	SEC Time	SDC Time	GBC Time	Model Time	MIP Gap (%)	Opt Pct (%)
	0.75	10.4	4.0	3.6	0.000	0.000	0.038	0.054	0.00	100
6	1	23.6	8.8	8.8	0.000	0.000	0.098	0.127	0.00	100
	1.25	27.6	16.2	13.4	0.000	0.000	0.146	0.187	0.00	100
Avg.		20.5	9.7	8.6	0.000	0.000	0.094	0.123	0.00	100
	0.75	31.6	16.2	9.8	0.000	0.000	0.161	0.223	0.00	100
8	1	41.6	22.4	14.2	0.000	0.001	0.249	0.311	0.00	100
	1.25	34.8	11.6	12.2	0.000	0.000	0.206	0.259	0.00	100
Avg		36.0	16.7	12.1	0.000	0.000	0.205	0.264	0.00	100
	0.75	127.6	89.0	32.6	0.001	0.002	0.777	0.878	0.00	100
10	1	87.6	39.6	26.6	0.001	0.001	0.714	0.787	0.00	100
	1.25	79.2	30.8	22.4	0.001	0.001	0.565	0.615	0.00	100
Avg		98.1	53.1	27.2	0.001	0.001	0.685	0.760	0.00	100
	0.75	133.2	44.6	23.8	0.001	0.001	0.829	0.894	0.00	100
12	1	151.6	100.4	28.0	0.001	0.003	0.900	1.006	0.00	100
	1.25	147.6	62.6	41.4	0.001	0.002	1.483	1.597	0.00	100
Avg		144.1	69.2	31.1	0.001	0.002	1.071	1.166	0.00	100
	0.75	262.0	84.2	38.6	0.002	0.003	1.818	1.993	0.00	100
14	1	187.2	70.8	22.2	0.002	0.002	1.075	1.344	0.00	100
	1.25	564.8	768.8	77.2	0.005	0.023	3.757	5.198	0.00	100
Avg		338.0	307.9	46.0	0.003	0.010	2.217	2.845	0.00	100
	0.75	371.6	185.6	38.4	0.004	0.006	2.042	2.535	0.00	100
16	1	667.6	247.2	124.0	0.007	0.010	7.221	8.228	0.00	100
	1.25	1172.8	792.6	352.0	0.013	0.032	21.702	28.442	0.00	100
Avg		737.3	408.5	171.5	0.008	0.016	10.321	13.068	0.00	100
	0.75	1017.2	1149.0	124.4	0.012	0.044	10.929	16.659	0.00	100
18	1	597.2	294.8	133.6	0.006	0.012	11.732	13.452	0.00	100
	1.25	1838.8	415.6	668.8	0.025	0.026	59.078	141.670	0.00	100
Avg		1151.1	619.8	308.9	0.014	0.027	27.247	57.261	0.00	100
	0.75	2151.6	3113.4	123.4	0.031	0.148	13.808	127.979	0.00	100
20	1	1140.0	628.4	318.6	0.015	0.031	35.045	54.026	0.00	100
	1.25	9496.8	3599.8	429.8	0.184	0.187	49.115	804.967	2.49	80
Avg		4262.8	2447.2	290.6	0.076	0.122	32.656	328.991	0.83	93
	0.75	1194.0	565.0	168.6	0.016	0.026	23.523	35.449	0.00	100
22	1	4888.4	1426.2	573.0	0.096	0.089	83.438	554.685	0.00	100
	1.25	6489.6	8880.4	1129.8	0.112	0.529	161.348	1268.469	1.97	80
Avg		4190.7	3623.9	623.8	0.075	0.215	89.436	619.534	0.66	93
	0.75	692.0	492.0	141.8	0.008	0.022	23.701	27.609	0.00	100
24	1	6674.4	4693.6	787.2	0.130	0.254	140.985	1622.960	2.81	60
	1.25	17027.2	13257.2	945.2	0.333	0.726	171.623	2900.182	8.95	20
Avg		8131.2	6147.6	624.7	0.157	0.334	112.103	1516.917	3.92	60
	0.75	19348.8	7383.2	408.4	0.510	0.546	83.768	1570.052	1.69	60
26	1	12798.8	11515.2	632.8	0.281	0.686	134.660	2206.446	5.31	40
	1.25	12745.6	11138.0	1064.8	0.236	0.675	227.720	3311.867	6.29	40
Avg		14964.4	10012.1	702.0	0.342	0.636	148.710	2362.789	4.43	47
	0.75	8915.6	9400.6	356.4	0.174	0.574	83.147	1960.745	1.65	80
28	1	5844.4	1775.6	837.4	0.135	0.153	199.365	1400.179	1.90	80
	1.25	18527.6	10192.2	1474.0	0.401	0.737	375.003	3470.617	7.16	20
Avg		11095.9	7122.8	889.3	0.237	0.488	219.172	2277.180	3.57	60
	0.75	8775.6	9480.0	513.2	0.162	0.718	150.546	1626.341	2.84	60
30	1	12975.6	13859.2	724.2	0.281	1.116	219.909	3246.540	5.22	20
	1.25	23480.4	12804.0	1072	0.489	0.883	336.829	3600.000	13.32	0
Avg		15077.2	12047.7	769.8	0.311	0.906	235.761	2824.564	7.13	27

cuts, and generalized Benders optimality cuts, as well as the associated separation times. We also collect the corresponding optimality gaps and the number of solved instances in percentage. All results are presented in Tables 2 and 3 for the 1-1 and M-M versions of PDTSPN, respectively.

The results of both types of instances share several similarities. First, the proposed approach can efficiently solve configurations with $n \leq 18$ to optimality, except for the case where $n = 18$ and $\ell = 1$. All the other instances under that size were solved within a minute on average. When the size becomes larger, some instances reach the time limit before closing the optimality gap. However, even for large instances such as $n = 20$ and 22, many were still solved to optimality as evidenced by the "Opt. Pct" column in both Tables 2 and 3. Second, we observe that the separation time spent on the general Benders cuts is significantly longer than the ones for supply-demand and subtour elimination cuts, which is expected as the former requires solving subproblem (4). Third, we notice that size of the instances grow, most of the algorithm running time is spent on solving the master problem (5).

In our implementation, the 1-1 PDTSPN instances are solved with the precedence constraints (11) added to the master problem (5). This leads to several performance differences when compared to the M-M PDTSPN case. First, in general, as shown in Tables 3 and 2 the M-M instances are solved faster than the 1-1 counterpart. Similarly, this trend is also apparent when comparing the MIP gaps and number of instances solved of the large instances. Second, in Table 3, there is a clear pattern showing that the instances with larger ℓ are more difficult to solve. Except for small instances where $n \leq 10$, the instances with $\ell = 1.25$ take much longer to solve than the others. This is mainly because larger areas potentially lead to more overlaps between the neighborhoods, which may produce many near-optimal solutions with different visiting sequences. However, this phenomenon is less apparent in Table 2. One explanation is that the one-to-one precedence constraints imposed in the master problem vastly reduce the number of feasible visiting sequences, which undermines the effects caused by the overlapped areas.

5.2 Experiment with Convex and Non-Convex Neighborhoods

5.2.1 Test Instances.

In this experiment, we consider each pair (n, α) with $n \in \{10, 12, \ldots, 18\}$ and $\alpha \in \{0, 0.1, 0.3, \ldots, 0.9\}$ as a configuration, where n is the number of neighborhoods, half of them being non-convex, and the parameter α, denoted the *fringe degree*, which is a parameter used to control the number of neighborhoods that are located near the perimeter of the area under consideration (see Figure 10). Specifically, we randomly generate the neighborhoods by locating their centers inside an annulus of radius range $[\alpha r, r]$. Thus, a small α allows the neighborhoods to spread throughout the area, whereas a large value tends to locate them in the periphery. The goal here is to analyze the effect of the separators based on the neighborhood's location. Intuitively, one would expect the effects of the separators to be more pronounced when more neighborhoods are on the outskirts of the given area, as it is more likely for the separators to slice through them. As for the previous experiments, we randomly generate five instances for each configuration (n, α) and report the average computational statistics in Table 4. To study the effects of adding the proposed BPC separators, we run each instance under two implementations: the cut generation approach with and without generating these separators.

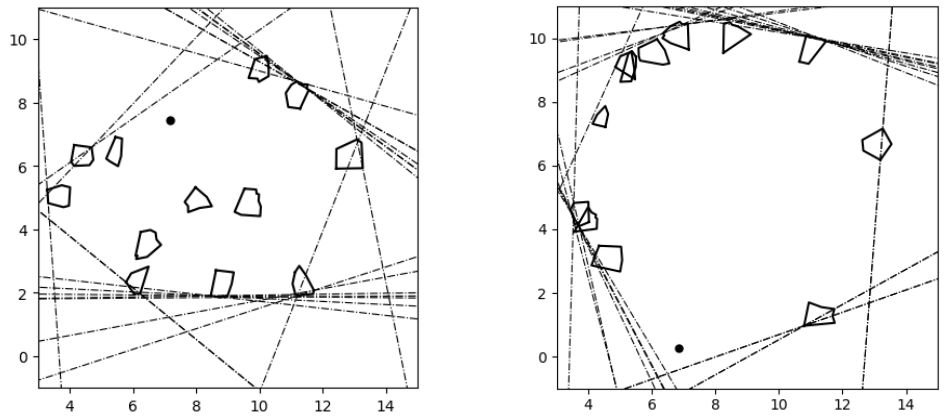

(a) Neighborhood fringe degree $\alpha = 0.1$ (b) Neighborhood fringe degree $\alpha = 0.9$

Figure 10: Illustration of separators for problems with convex and non-convex neighborhoods. All the convex neighborhoods are represented by the intersection of half-planes, and the non-convex neighborhoods use the representation introduced in Section 4.3. The fringe degree parameter α controls how close the neighborhoods are to the outskirts of the area. For a small α as in (a), neighborhoods can spread across the area; for a large α as in (b), neighborhoods are located near the area's periphery.

5.2.2 BPC Separator Generation.

To generate separators, we use a variant of Algorithm 1 for our non-convex representation. Because the subproblem $\Phi(u)$ in this experiment has binary variables indicating the boundary segments of the neighborhoods, the benefits of using BPC separators is to reduce the number of these binary variables or even transform some non-convex neighborhoods into convex. For instance, the non-convex neighborhood located at $(7.5, 10)$ in Figure 10b becomes convex after removing the redundant area using the generated separators. However, applying Algorithm 1 naively may, on the contrary, even increase the number of boundary segments. To avoid this, we check whether any pair of non-consecutive points in each neighborhood can induce a non-trivial BPC separator, i.e., separators that remove nonempty areas. Every separator produced by this procedure will decrease the number of boundary segments by at least one, which in turn reduces the total number of binary variables in the subproblem $\Phi(u)$.

5.2.3 Experiment Results.

In Table 4, we report the aggregated results from each configuration under the Benders decomposition implementation with and without the separators. A bold font indicates a better performance in the associated configuration. The first observation is that, unsurprisingly, these instances are more difficult than the 1-1 and M-M instances having only convex neighborhoods as the model runtimes listed in Table 4 are longer than the ones reported in Table 2 and 3 from instances of comparable sizes. This prolonged runtime is mainly caused by the increased complexity in the subproblem $\Phi(u)$ for generating the Benders optimality cuts.

Perhaps the most important observation is that the BPC separators help reduce the overall runtime in 20 out of 25 configurations used. The running times are longer for configurations $(10, 0.3)$, $(12, 0.1)$, $(12, 0.3)$, $(14, 0.3)$, and $(18, 0.7)$. In such cases, the extra runtime accounts for about 12% on average. In contrast, the runtime reduction enhanced by the separators is significant under many configurations. For

Table 4: Results for the generalized Benders decomposition approach on instances with non-convex neighborhoods. For each configuration, we report the average model runtime in seconds (Model Time), average number of generalized Benders optimality cuts (Num. GBCs), average number of binary decision variables in the subproblems (Num. BDVs), and the average runtime of the subproblems in seconds (Sp Time) for implementations with and without the separators. We use the bold font to indicate a better performance.

Config		Model Time			Num. GBCs		Num. BDVs		Sp Time	
n	α	W/O Seps	W/ Seps	Dec Pct (%)	W/O Seps	W/ Seps	W/O Seps	W/ Seps	W/O Seps	W/ Seps
10	0.1	5.418	**4.826**	10.9	**45.8**	47.3	40.0	**29.0**	0.138	**0.135**
	0.3	**2.913**	3.298	−13.2	**21.2**	25.2	37.4	**27.4**	0.157	**0.122**
	0.5	4.973	**4.895**	1.6	26.0	**25.4**	41.0	**28.2**	0.146	**0.141**
	0.7	3.981	**2.523**	36.6	24.6	**17.6**	41.0	**28.2**	0.135	**0.132**
	0.9	3.856	**1.928**	50.0	23.8	**16.0**	41.4	**21.8**	0.155	**0.110**
Avg.		4.179	**3.439**	17.7	27.5	**25.4**	40.2	**26.8**	0.146	**0.128**
12	0.1	**15.811**	20.060	−26.9	**55.0**	65.2	48.2	**34.0**	0.269	**0.258**
	0.3	**15.765**	18.826	−19.4	**64.8**	67.8	49.6	**38.4**	0.267	**0.263**
	0.5	22.775	**13.946**	38.8	61.2	**55.0**	47.2	**32.4**	0.350	**0.255**
	0.7	15.449	**10.560**	31.6	41.0	**37.8**	47.8	**39.2**	0.395	**0.327**
	0.9	31.036	**24.937**	19.7	88.6	**83.4**	46.8	**34.0**	0.348	**0.265**
Avg.		20.167	**17.666**	12.4	62.1	**61.8**	47.9	**35.6**	0.326	**0.273**
14	0.1	117.642	**88.599**	24.7	158.2	**138.2**	56.2	**47.4**	0.701	**0.615**
	0.3	**29.622**	32.895	−11.0	**59.0**	59.8	56.2	**46.4**	**0.504**	0.512
	0.5	247.207	**132.756**	46.3	154.2	**123.0**	57.8	**49.8**	1.071	**0.867**
	0.7	56.007	**49.708**	11.2	53.0	**49.0**	56.4	**43.2**	0.905	**0.806**
	0.9	50.660	**34.848**	31.2	74.6	**60.2**	52.6	**42.0**	0.622	**0.533**
Avg.		100.228	**67.761**	32.4	99.8	**86.0**	55.8	**45.8**	0.761	**0.667**
16	0.1	856.973	**764.187**	10.8	**391.0**	396.4	65.0	**57.0**	2.036	**1.583**
	0.3	129.955	**108.475**	16.5	**116.8**	146.8	64.0	**49.0**	0.983	**0.677**
	0.5	625.837	**484.716**	22.5	392.8	**356.4**	64.8	**53.2**	1.486	**1.246**
	0.7	595.725	**525.465**	11.8	**210.6**	213.6	62.6	**53.8**	2.840	**2.243**
	0.9	571.142	**431.121**	24.5	307.8	**281.0**	62.8	**53.4**	2.296	**1.517**
Avg.		555.926	**462.793**	16.8	283.8	**278.8**	63.8	**53.3**	1.928	**1.453**
18	0.1	2286.941	**1908.548**	16.5	504.6	**427.8**	70.6	**65.8**	16.972	**13.461**
	0.3	2930.376	**1891.554**	35.5	**604.6**	704.6	70.4	**57.6**	5.454	**2.757**
	0.5	2319.071	**1965.479**	15.2	**755.0**	1005.4	71.6	**57.6**	5.835	**2.707**
	0.7	**889.397**	990.379	−11.4	**323.6**	350.6	71.4	**56.8**	2.590	**2.572**
	0.9	1768.116	**1471.026**	16.8	**285.0**	307.0	71.2	**59.8**	6.289	**4.556**
Avg.		2038.780	**1645.397**	19.3	**494.6**	559.1	71.0	**59.5**	7.428	**5.211**

instance, in $(10, 0, 7)$, $(10, 0, 9)$, $(12, 0, 5)$, $(12, 0, 7)$, $(14, 0, 5)$, $(14, 0, 9)$, $(18, 0, 3)$, the overall model runtimes have been reduced by more than 30%. A close investigation of column Num. GBCs shows that the main reason causing the extra runtime in using the separators in those rare cases is the additional number of subproblems for generating the GBCs. Indeed, suppose we only focus on the average runtime for the subproblems $\Phi(u)$. Except for one configuration $(14, 0.3)$, the implementation with the separators always dominates the one without the separators, which is expected since the BPC separators can reduce the number of binary decision variables in the subproblems (see column Num. BDVs). Furthermore, there is a positive correlation between the fringe degree and the percentage of reduced binary decision variables. One possible explanation is that with a higher fringe degree, non-convex neighborhoods are more likely to generate BPC separators, as illustrated in Figure 10.

Overall, this experiment demonstrates that, when the subproblem becomes difficult, special BPC separator generation subroutines can be designed using the optimality conditions introduced in Section 3 to enhance the computational performance for solving the PDTSPN instances.

6 Concluding Remarks

In this paper we studied a variant of the traveling salesman problem called the pickup-and-delivery traveling salesman problem with neighborhoods, which combines the main characteristics of the pickup and delivery TSP and the TSP with neighborhoods.

First, we derived two optimality conditions for PDTSPN with compact neighborhoods that can have arbitrary shapes. The first condition characterizes whether a given tour is locally optimal at the visiting point of each neighborhood. The second condition states that every boundary-projection-closed separator contains all the non-redundant optimal tours. Hence, the intersection of these separators, defined as the domination hull, can be used to cut off sub-optimal regions of the neighborhoods. We also developed a binary-search-based algorithm to approximate the domination hull efficiently.

Next, we proposed a mixed-integer nonlinear programming formulation to solve PDTSPN on instances with convex and non-convex neighborhoods. A cut-generation solution approach was developed based on the generalized Benders decomposition. This approach iterates between two models: a master problem that identifies a feasible visiting sequence and a subproblem that searches for an optimal visiting location under the given sequence. We adapted this method to tackle instances with different supply-demand precedence relationships, including the 1-1, 1-M-1, and M-M versions.

Finally, we conducted an extensive set of computational experiments to test the proposed solution approach on a wide variety of instances. Our experiments showed that a small number of separators is sufficient to trim a large portion of the neighborhoods, and this effectiveness in size reduction translates to the runtime efficiency when the subproblem $\Phi(u)$ is relatively difficult. Also the experiments evidenced that our solution approach works efficiently on most of the tested instances.

Due to the generality of the proposed optimality conditions and solution approaches, we can extend them to other TSPN-related problems that may even involve non-convex neighborhoods.

References

N. Agatz, P. Bouman, and M. Schmidt. Optimization approaches for the traveling salesman problem with drone. *Transportation Science*, 52(4):965–981, 2018.

S. Anily and G. Mosheiov. The traveling salesman problem with delivery and backhauls. *Operations Research Letters*, 16(1):11–18, 1994.

E. M. Arkin and R. Hassin. Approximation algorithms for the geometric covering salesman problem. *Discrete Applied Mathematics*, 55(3):197–218, 1994.

M. Battarra, J.-F. Cordeau, and M. Iori. Chapter 6: pickup-and-delivery problems for goods transportation. In *Vehicle Routing: Problems, Methods, and Applications, Second Edition*, pages 161–191. Society for Industrial and Applied Mathematics, 2014.

B. Behdani and J. C. Smith. An integer-programming-based approach to the close-enough traveling salesman problem. *INFORMS Journal on Computing*, 26(3):415–432, 2014.

E. Belongia. The funcol program for primary health care, colombia. *Cultural Survival Quarterly*, 12(1), 1988.

G. Berbeglia, J.-F. Cordeau, I. Gribkovskaia, and G. Laporte. Static pickup and delivery problems: a classification scheme and survey. *Top*, 15(1):1–31, 2007.

G. Berbeglia, J.-F. Cordeau, and G. Laporte. Dynamic pickup and delivery problems. *European Journal of Operational Research*, 202(1):8–15, 2010.

F. Carrabs, C. Cerrone, R. Cerulli, and M. Gaudioso. A novel discretization scheme for the close enough traveling salesman problem. *Computers & Operations Research*, 78:163–171, 2017.

N. Christofides. Worst-case analysis of a new heuristic for the travelling salesman problem. Technical report, Carnegie-Mellon University, Pittsburgh PA, USA, 1976.

J.-F. Cordeau, M. Dell'Amico, and M. Iori. Branch-and-cut for the pickup and delivery traveling salesman problem with FIFO loading. *Computers & Operations Research*, 37(5):970–980, 2010a.

J.-F. Cordeau, M. Iori, G. Laporte, and J. J. Salazar González. A branch-and-cut algorithm for the pickup and delivery traveling salesman problem with LIFO loading. *Networks*, 55(1):46–59, 2010b.

W. P. Coutinho, R. Q. d. Nascimento, A. A. Pessoa, and A. Subramanian. A branch-and-bound algorithm for the close-enough traveling salesman problem. *INFORMS Journal on Computing*, 28(4):752–765, 2016.

M. Dell'Amico, R. Montemanni, and S. Novellani. Drone-assisted deliveries: New formulations for the flying sidekick traveling salesman problem. *Optimization Letters*, 15(5):1617–1648, 2021.

A. Dumitrescu and J. S. Mitchell. Approximation algorithms for TSP with neighborhoods in the plane. *Journal of Algorithms*, 48(1):135–159, 2003.

I. Dumitrescu, S. Ropke, J.-F. Cordeau, and G. Laporte. The traveling salesman problem with pickup and delivery: polyhedral results and a branch-and-cut algorithm. *Mathematical Programming*, 121(2):269–305, 2010.

Y. Emami, K. Li, and E. Tovar. Buffer-aware scheduling for UAV relay networks with energy fairness. In *2020 IEEE 91st Vehicular Technology Conference (VTC2020-Spring)*, pages 1–5, 2020.

M. Gendreau, G. Laporte, and D. Vigo. Heuristics for the traveling salesman problem with pickup and delivery. *Computers & Operations Research*, 26(7):699–714, 1999.

A. M. Geoffrion. Generalized Benders decomposition. *Journal of Optimization Theory and Applications*, 10 (4):237–260, 1972.

I. Gribkovskaia, Ø. Halskau sr., G. Laporte, and M. Vlček. General solutions to the single vehicle routing problem with pickups and deliveries. *European Journal of Operational Research*, 180(2):568–584, 2007.

J. Gudmundsson and C. Levcopoulos. A fast approximation algorithm for TSP with neighborhoods. *Nordic Journal of Computing*, 6(4):469–488, 1999.

D. J. Gulczynski, J. W. Heath, and C. C. Price. The close enough traveling salesman problem: A discussion of several heuristics. In *Perspectives in Operations Research*, pages 271–283. Springer, 2006.

H. Hernández-Pérez and J.-J. Salazar-González. A branch-and-cut algorithm for a traveling salesman problem with pickup and delivery. *Discrete Applied Mathematics*, 145(1):126–139, 2004a.

H. Hernández-Pérez and J.-J. Salazar-González. Heuristics for the one-commodity pickup-and-delivery traveling salesman problem. *Transportation Science*, 38(2):245–255, 2004b.

H. Hernández-Pérez, I. Rodríguez-Martín, and J. J. Salazar-González. A hybrid GRASP/VND heuristic for the one-commodity pickup-and-delivery traveling salesman problem. *Computers & Operations Research*, 36(5):1639–1645, 2009.

H. Hernández-Pérez and J.-J. Salazar-González. The multi-commodity one-to-one pickup-and-delivery traveling salesman problem. *European Journal of Operational Research*, 196(3):987–995, 2009. ISSN 0377-2217.

B. Kalantari, A. V. Hill, and S. R. Arora. An algorithm for the traveling salesman problem with pickup and delivery customers. *European Journal of Operational Research*, 22(3):377–386, 1985.

K. Li, W. Ni, E. Tovar, and A. Jamalipour. On-board deep Q-network for UAV-assisted online power transfer and data collection. *IEEE Transactions on Vehicular Technology*, 68(12):12215–12226, 2019.

C. S. Mata and J. S. Mitchell. Approximation algorithms for geometric tour and network design problems. In *Proceedings of the Eleventh Annual Symposium on Computational Geometry*, pages 360–369, 1995.

D. Mavalankar. Doctors for tribal areas: Issues and solutions. *Indian Journal of Community Medicine: Official Publication of Indian Association of Preventive & Social Medicine*, 41(3):172, 2016.

W. K. Mennell. *Heuristics for solving three routing problems: Close-enough traveling salesman problem, close-enough vehicle routing problem, and sequence-dependent team orienteering problem*. University of Maryland, College Park, MD, USA, 2009.

N. Mladenović, D. Urošević, and A. Ilić. A general variable neighborhood search for the one-commodity pickup-and-delivery traveling salesman problem. *European Journal of Operational Research*, 220(1):270–285, 2012.

G. Mosheiov. The travelling salesman problem with pick-up and delivery. *European Journal of Operational Research*, 79(2):299–310, 1994.

C. C. Murray and A. G. Chu. The flying sidekick traveling salesman problem: Optimization of drone-assisted parcel delivery. *Transportation Research Part C: Emerging Technologies*, 54:86–109, 2015.

R. J. O'Neil and K. Hoffman. Exact methods for solving traveling salesman problems with pickup and delivery in real time. *Technical Report. George Mason University. 4400 University Dr., Fairfax, VA*, 9, 2017.

F. Ono, H. Ochiai, and R. Miura. A wireless relay network based on unmanned aircraft system with rate optimization. *IEEE Transactions on Wireless Communications*, 15(11):7699–7708, 2016.

S. N. Parragh, K. F. Doerner, and R. F. Hartl. A survey on pickup and delivery problems. *Journal für Betriebswirtschaft*, 58(2):81–117, 2008.

H. N. Psaraftis. Analysis of an $o(n^2)$ heuristic for the single vehicle many-to-many euclidean dial-a-ride problem. *Transportation Research Part B: Methodological*, 17(2):133–145, 1983.

Y. Qu and J. F. Bard. A branch-and-price-and-cut algorithm for heterogeneous pickup and delivery problems with configurable vehicle capacity. *Transportation Science*, 49(2):254–270, 2015.

K. Ramalingareddy. Improving health services for tribal populations. *International Journal of Research in Social Sciences*, 6(11):345–357, 2016.

J. Renaud, F. F. Boctor, and J. Ouenniche. A heuristic for the pickup and delivery traveling salesman problem. *Computers & Operations Research*, 27(9):905–916, 2000.

S. Ropke and D. Pisinger. An adaptive large neighborhood search heuristic for the pickup and delivery problem with time windows. *Transportation science*, 40(4):455–472, 2006.

M. W. Savelsbergh and M. Sol. The general pickup and delivery problem. *Transportation science*, 29(1): 17–29, 1995.

P. Toth and D. Vigo. *The vehicle routing problem*. Society for Industrial and Applied Mathematics, 2002.

M. Veenstra, K. J. Roodbergen, I. F. Vis, and L. C. Coelho. The pickup and delivery traveling salesman problem with handling costs. *European Journal of Operational Research*, 257(1):118–132, 2017.

X. Wang, B. Golden, and E. Wasil. A steiner zone variable neighborhood search heuristic for the close-enough traveling salesman problem. *Computers & Operations Research*, 101:200–219, 2019.

N. Wei, J. L. Walteros, M. R. Worden, and H. J. Ortiz-Peña. A resiliency analysis of information distribution policies over mobile ad hoc networks. *Optimization Letters*, 15(4):1081–1103, 2021.

H. Xu, Z.-L. Chen, S. Rajagopal, and S. Arunapuram. Solving a practical pickup and delivery problem. *Transportation science*, 37(3):347–364, 2003.

B. Yuan, M. Orlowska, and S. Sadiq. On the optimal robot routing problem in wireless sensor networks. *IEEE Transactions on Knowledge and Data Engineering*, 19(9):1252–1261, 2007.

F. Zhao, S. Li, J. Sun, and D. Mei. Genetic algorithm for the one-commodity pickup-and-delivery traveling salesman problem. *Computers & Industrial Engineering*, 56(4):1642–1648, 2009.

7 Mathematical Proofs

We present all mathematical proofs in this section.

Proof. Proof of Proposition 1. Given the problem's setting, each neighborhood except U_0 has either $d_i > 0$ or $s_i > 0$. Hence, to satisfy all the pickup and delivery requirements, the vehicle needs to visit each neighborhood at least once. For the first claim, all is left to show is that there exists an optimal tour that visits each neighborhood at most once. Notice that the problem is feasible by the first statement in Assumption 1 and the optimality is always obtainable due to the compactness of all the neighborhoods. So, we can start with an arbitrarily selected optimal tour γ that is represented by the sequence $(p_0, p_1, p_2, \cdots, p_n)$, i.e., a closed tour that starts and ends at p_0 and traverses from p_1 to p_n in between, where every point p_k belongs to some neighborhood U_i that may have been visited more than once. We call the number of visits to a neighborhood U_i in this sequence the multiplicity of U_i. If the multiplicity of every neighborhood is one in γ, we are done. Now, suppose otherwise, then the following procedure will reduce by one the multiplicity of any neighborhood that has been visited repeatedly in γ. By applying this process as many times as necessary, one can produce an optimal tour that is Hamiltonian, thus proving the claim.

The procedure is as follows. If a neighborhood that has been visited multiple times, say neighborhood U_i, is a demand neighborhood, then we use p_k and $p_{k'}$ to denote the points in γ that visit U_i the first two times, and let l_k and $l_{k'}$ be the corresponding delivered commodities during each visit. Then, we split the tour γ into several subpaths as

$$\gamma = (p_0 \rightsquigarrow p_{k-1} \to p_k \to p_{k+1} \rightsquigarrow p_{k'} \rightsquigarrow p_n),$$

where "$\to$" means no other neighborhoods are visited in between and "$\rightsquigarrow$" indicates that potentially multiple neighborhoods are visited in between. We construct the following new tour

$$\gamma' = (p_0 \rightsquigarrow p_{k-1} \to p_{k+1} \rightsquigarrow p_{k'} \rightsquigarrow p_n).$$

Let v, v' be two vehicles following tours γ and γ', respectively. Comparing with v, vehicle v' will only take two different actions in tour γ': it skips the stop p_k and it drops $l_k + l_{k'}$ commodities at point $p_{k'}$. By this design, before the point p_{k-1} and after the point $p_{k'}$, the two vehicles are at the same state in their routes, i.e., at each fixed time, they are at the same location with the same amount of commodities. For the tour between p_{k-1} and $p_{k'}$, it is obvious that the second tour is no longer than the first tour (in fact, they have the same length since γ is assumed to be optimal). We only need to show this new construction is possible between p_{k+1} and $p_{k'}$. Notice at the time of reaching p_{k+1}, vehicle v holds strictly less commodities than vehicle v'. Along with the second statement in Assumption 1, it is clear that v' can always replicate the actions that v takes in the subpath between p_{k+1} and $p_{k'}$. Thus, we have reduced the multiplicity of the neighborhood U_i by one in this case. A similar procedure and argument can be applied to the case that the repeatedly visited neighborhood is a supply neighborhood. So, we proved the first claim.

Therefore, we can focus on all the tours that visit each neighborhood exactly once. That consists of all the closed tours that pass through some point set $\{p_i\}_{i \in I}$ with $p_i \in U_i$ for all $i \in I$. Now, because the shortest closed tour for each such fixed point set $\{p_i\}_{i \in I}$ is a Hamiltonian tour, so is the global optimal tour

among all the possible point sets. □

Proof. Proof of Lemma 1. $\mathcal{U}_k = \varnothing$ implies either that no neighborhood contains p_k or, if one does, say U_i, then U_i is also intersected by the complement path $\bar{P}_k$. Clearly, in both cases, the sequence $\gamma' = (p_0, \ldots, p_{k-1}, p_{k+1}, \ldots, p_n)$ also visits U_i. Moreover, p_k being a turning point implies that γ' is strictly shorter than the original optimal sequence, which leads to a contradiction. □

Proof. Proof of Theorem 1. We prove the first statement by contradiction. Let p_k be a turning point such that all neighborhoods $U_i \in \mathcal{U}_k$ intersect with P_k at more points than just p_k. Then, we will construct a strictly shorter feasible sequence γ' that still visits all the neighborhoods, which contradicts the optimality of γ^*. Let p_{k-1} and p_{k+1} be the previous and next points of p_k in γ^*, and let $[p_{k-1}, p_k)$ and $(p_k, p_{k+1}]$ represent the half-open line segment between the two endpoints. For each $U_i \in \mathcal{U}_k$, we define two sets

$$L_i = \arg \max_{p \in U_i \cap [p_{k-1}, p_k)} \delta(p, p_k),$$
$$R_i = \arg \max_{p \in U_i \cap (p_k, p_{k+1}]} \delta(p, p_k).$$

Thus, L_i (or R_i) contains the points in the intersection of U_i and the segment $[p_{k-1}, p_k)$ (or $(p_k, p_{k+1}]$) that is the farthest to point p_k. Notice that, L_i (or R_i) is either a singleton or an empty set, but $L_i \cup R_i$ must be nonempty by the choice of U_i. Then, we define the following two sets

$$L = \arg \min_{p \in \bigcup_{i \in I_k} L_i} \delta(p, p_k),$$
$$R = \arg \min_{p \in \bigcup_{i \in I_k} R_i} \delta(p, p_k),$$

where I_k is the index set of the neighborhoods in $\mathcal{U}_k$. Thus, L (or R) contains the points that are closest to p_k among all the points in the union $\bigcup_{i \in I_k} L_i$ (or $\bigcup_{i \in I_k} R_i$). By the assumption on all U_i's, $L \cup R \neq \varnothing$. Thus, we are left with three possible cases. In the first case, we have $L = \varnothing$ and $R \neq \varnothing$. This means each $U_i \in \mathcal{U}_k$ intersects some point in $(p_k, p_{k+1}]$. Take any $r \in R$, we construct a feasible sequence $\gamma' = (p_0, \ldots, p_{k-1}, r, p_{k+1}, \ldots, p_n)$, which replaces p_k with r. In the second case, $L \neq \varnothing$ but $R = \varnothing$. Similarly, we construct γ' by replacing p_k with l for any $l \in L$. In the last case, both L and R are nonempty. Then, we define $\gamma' = (p_0, \ldots, p_{k-1}, l, r, p_{k+1}, \ldots, p_n)$ for $l \in L$ and $r \in R$. In all three cases, it is easy to check that the new sequence γ' covers all the neighborhoods in $\mathcal{U}_k$ by the construction and is strictly shorter than γ^* by Lemma 2, which contradicts that γ^* is optimal. Hence, we proved the first claim.

For the second statement, suppose every $U_i \in \mathcal{U}_k$ intersects the triangle T_k at some point $q_i \neq p_k$. Then, we can partition the neighborhoods in $\mathcal{U}_k$ into two groups $\mathcal{U}_k^1$ and $\mathcal{U}_k^2$.The former contains neighborhoods that have a path $q_i \rightsquigarrow p_k$ inside the inner region enclosed by the closed curve γ^*; the latter includes all the rest neighborhoods, each of which must have a path $q_i \rightsquigarrow p_k$ intersects the path P_k, because, otherwise, they must have a path $q_i \rightsquigarrow p_k$ intersects the complement path $\bar{P}_k$, which makes U_i non-active by Definition 3, a contradiction. Notice that $\mathcal{U}_k^1$ is nonempty, otherwise, all neighborhoods in $\mathcal{U}_k$ intersect P_k, which contradicts

the first statement we have just shown. For each $U_i \in \mathcal{U}_k^1$, let ω_i be a path connecting q_i to p_k and is inside the inner region enclosed by γ^*, and let C_ϵ be a circle of radius ϵ centered at p_k. Then, for a sufficiently small scalar $\epsilon > 0$, the circle C_ϵ intersects all the paths ω_i's as well as the half open line segments $[p_{k-1}, p_k)$ and $(p_k, p_{k+1}]$. We use l and r to denote the intersection points of C_ϵ with $[p_{k-1}, p_k)$ and $(p_k, p_{k+1}]$, respectively. Then, the new sequence $\gamma' = (p_0, \ldots, p_{k-1}, l, r, p_{k+1}, \ldots, p_n)$ visits all the neighborhoods in $\mathcal{U}_k^1$ since the line segment $[l, r]$ intersects all the paths ω_i's. Moreover, for a sufficiently small $\epsilon > 0$, γ' also intersects all neighborhoods in $\mathcal{U}_k^2$, since the intersection points of each neighborhood $U_i \in \mathcal{U}_k^2$ and the path P_k have a fixed positive distance to p_k. Furthermore, the new curve γ' is strictly shorter than γ^* by the construction and the triangle inequality, which contradicts the optimality of γ^*. □

Proof. Proof of Corollary 1. Because all neighborhoods are disjoint, each turning point can belong to exactly one U_i. This shows that $\mathcal{U}_k$ contains only one neighborhood. By the first statement of Theorem 1, $U_i \cap P_k = \{p_k\}$. Suppose U_i also intersects T_k at some point $q_i \neq p_k$. By Lemma 2, replacing q_i with p_k in γ^* produces a strictly shorter feasible sequence, which is a contradiction. □

Proof. Proof of Theorem 2. Let $\mathbf{p} = (p_i)_{i \in I_0}$ be the local optimal curve γ_σ^*, where $p_i \in U_i$ for each $i \in I_0$ and p_i is either a turning or a passing point. Without loss of generality, we assume that the index set I_0 is sorted by the visiting order σ. We use $\hat{\mathbf{p}}$ to denote the corresponding point set $\{p_i\}_{i \in I_0}$. Clearly, if $\hat{\mathbf{p}} \subseteq H$, then the entire tour γ_σ^* also lies within the half-plane H. Suppose otherwise that $\hat{\mathbf{p}} \not\subseteq H$. Then, there are two possible cases: either all or part of the points in $\hat{\mathbf{p}}$ lie in the complement of H.

In the former case, we claim that the projected tour $\mathrm{proj}_H(\mathbf{p}) = (\mathrm{proj}_H(p_i))_{i \in I_0}$ visits every neighborhood U_i in the order of σ and is strictly shorter than γ_σ^*, which induces a contradiction. By assumption, γ_σ^* does not lie in a straight line that parallels to ∂H, which implies the projection of γ_σ^* onto ∂H is strictly shorter than γ_σ^*. It is left to show that $\mathrm{proj}_H(p_i) \in U_i$ for each $i \in I_0$. If the point p_i is on the boundary of U_i, then $\mathrm{proj}_H(p_i) \in U_i$ is true due to H is a BPC separator of U_i. Otherwise, p_i is an interior point of U_i. Then, the line extended from the line segment $[\mathrm{proj}_H(p_i), p_i]$ intersects U_i at some point $p_i' \in \partial U_i \setminus H$. Then, we have $\mathrm{proj}_H(p_i) = \mathrm{proj}_H(p_i') \in U_i$, where the equality is by the construction of p_i' and the membership relation is due to H is a BPC separator of U_i.

In the latter case, some point $p_0 \in \hat{\mathbf{p}}$ is in the half-plane H. Then, we represent γ_σ^* as a continuous function from the closed interval $[0, 1]$ to $\mathbb{R}^2$ such that $\gamma_\sigma^*(0) = \gamma_\sigma^*(1) = p_0$, and $\gamma_\sigma^*(t_i) = p_i$ for all $i \in I_0$. By assumption, there is also some point in $\hat{\mathbf{p}}$ that is not in H, i.e., $\gamma_\sigma^*(t_i) \notin H$ for some $i \in I$, where I is the index set $I_0 \setminus \{0\}$. The fact that γ_σ^* is a continuous function means there exists some closed neighborhood $T = [t_{\min}, t_{\max}] \subseteq [0, 1]$ of t_i such that the path $\gamma_\sigma^*(T)$ intersects H only at the two endpoints $p_{\min} = \gamma_\sigma^*(t_{\min})$ and $p_{\max} = \gamma_\sigma^*(t_{\max})$. Let $T' = (t_{\min}, t_{\max})$ be the corresponding open interval of T, and we use the set $I' = \{i \in I \mid t_i \in T'\}$ to label all the neighborhoods that are visited by the path $\gamma_\sigma^*(T')$. Then, we consider the following projected sequence

$$\mathrm{proj}_H(\gamma_\sigma^*(T)) = (p_{\min}, (\mathrm{proj}_H(p_i))_{i \in I'}, p_{\max}) .$$

This sequence represents a subtour that visits all the neighborhoods $\{U_i\}_{i\in I'}$ with the same visiting order since H is a BPC separator of $\mathcal{U}$. Also, $\text{proj}_H(\gamma^*_\sigma(T))$ is strictly shorter than the original segment $\gamma^*_\sigma(T)$ since the tour is non-redundant. Moreover, $\text{proj}_H(\gamma^*_\sigma(T))$ and $\gamma^*_\sigma(T)$ shares the same endpoints. Thus, replacing the subtour $\gamma^*_\sigma(T)$ in γ^*_σ with the projected sequence produces a strictly shorter feasible solution, which yields a contradiction. □

Proof. Proof of Corollary 2. By Theorem 2, given that some optimal curve γ^* is non-redundant, then γ^* lies in $D_{\mathcal{U}}$, which shows $D_{\mathcal{U}}$ is nonempty. $D_{\mathcal{U}}$ is convex and closed since it is the intersection of a set of half-planes. Finally, by definition, a sufficiently large polygon that contains all the neighborhoods can be produced by the intersection of a set of BPC separators. Thus, it also contains $D_{\mathcal{U}}$, which means $D_{\mathcal{U}}$ is bounded, which entails compactness. □

Proof. Proof of Proposition 2. Given the initial input $(0, r, \theta, \mathcal{U})$, it suffices to show that, for any value $c \in (0, r)$, if $H_{\theta,c}$ is a BPC separator, then so is $H_{\theta,b}$ for all $b \in (c, r]$; if $H_{\theta,c}$ is not a BPC separator, neither is $H_{\theta,a}$ for all $a \in [0, c)$. To prove the former, we suppose $H_{\theta,c}$ is a BPC separator of $\mathcal{U}$, i.e., it is a BPC separator for every $U \in \mathcal{U}$. Take any $U \in \mathcal{U}$ and $b \in (c, r]$, the boundary points that are not contained in the half-plane $H_{\theta,b}$ is denoted by $\partial U \setminus H_{\theta,b}$. Clearly, we have the following

$$\partial U \setminus H_{\theta,b} \subseteq \partial U \setminus H_{\theta,c}.$$

Hence, for every $p \in \partial U \setminus H_{\theta,b}$, the projection $\text{proj}_{H_{\theta,c}}(p)$ is inside U, since $H_{\theta,c}$ is BPC separator of U by assumption. Moreover, because $H_{\theta,b}$ is parallel to $H_{\theta,c}$, the line segment $[p, \text{proj}_{H_{\theta,c}}(p)]$ intersects the line $\partial H_{\theta,b}$ at the projection point $\text{proj}_{H_{\theta,b}}(p)$. Thus, $\text{proj}_{H_{\theta,b}}(p) \in U$ due to the convexity of U, which shows $H_{\theta,b}$ is a BPC separator of U by definition. For the latter statement, we take any $a \in [0, c)$ and assume $H_{\theta,c}$ is not a BPC separator of $\mathcal{U}$. That is, for some $U \in \mathcal{U}$, $H_{\theta,c}$ is not a BPC separator of U. This means for some point $p \in \partial U \setminus H_{\theta,c}$, the projection $\text{proj}_{H_{\theta,c}}(p)$ is not in U. Same as before, the point p belongs to $\partial U \setminus H_{\theta,a}$. Towards a contradiction, suppose $H_{\theta,a}$ is a BPC separator of $\mathcal{U}$, then $\text{proj}_{H_{\theta,a}}(p) \in U$. Same as before, the segment $[p, \text{proj}_{H_{\theta,a}}(p)]$ intersects the line $\partial H_{\theta,c}$ at the projection point $\text{proj}_{H_{\theta,c}}(p)$. Then, the convexity of U implies $\text{proj}_{H_{\theta,c}}(p) \in U$, which contradicts the choice of p. This concludes the proof. □

Proof. Proof of Proposition 3. Every $u \in E_{sd}$ represents a feasible sequence of neighborhoods. Hence, after solving the corresponding subproblem $\Phi(u)$ optimally, the right-hand-side of new constraint (7) enforces the actual length of the shortest Hamiltonian tour under the given sequence u. Therefore, regardless of the convexity of (3f), the GBCs from (7) yield a sharp underestimator θ of the tour lenght, which guarantees the correctness of the cut generation method from the classic upper and lower bounding argument of the Benders decomposition. □